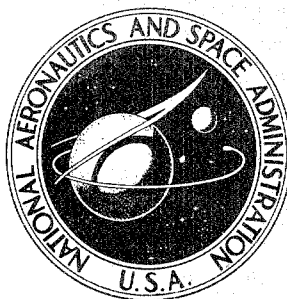


NASA CONTRACTOR  
REPORT



NASA CR-1367

NASA CR-1367

19960516 054

DISTRIBUTION STATEMENT A

Approved for public release;  
Distribution Unlimited

ELECTRICAL CHARACTERISTICS  
OF PYRRONE POLYMERS

*by P. J. Reucroft, H. Scott, P. L. Kronick,  
and F. L. Serafin*

*Prepared by*  
FRANKLIN INSTITUTE RESEARCH LABORATORIES  
Philadelphia, Pa.  
*for Langley Research Center*

DTIC QUALITY INSPECTED 1

NATIONAL AERONAUTICS AND SPACE ADMINISTRATION • WASHINGTON, D. C. • JUNE 1969

DEPARTMENT OF DEFENSE  
PLASTICS TECHNICAL EVALUATION CENTER  
PICATINNY ARSENAL, DOVER, N. J.

PLASTIC 12341

NASA CR-1367

## ELECTRICAL CHARACTERISTICS OF PYRRONE POLYMERS

By P. J. Reucroft, H. Scott, P. L. Kronick, and F. L. Serafin

Distribution of this report is provided in the interest of information exchange. Responsibility for the contents resides in the author or organization that prepared it.

Prepared under Contract No. NAS 1-7408 by  
FRANKLIN INSTITUTE RESEARCH LABORATORIES  
Philadelphia, Pa.

for Langley Research Center

NATIONAL AERONAUTICS AND SPACE ADMINISTRATION

---

For sale by the Clearinghouse for Federal Scientific and Technical Information  
Springfield, Virginia 22151 - CFSTI price \$3.00

DTIC QUALITY INSPECTED 4

## TABLE OF CONTENTS

	<u>Page</u>
1. INTRODUCTION	1
2. EXPERIMENTAL	1
2.1 PREPARATION OF MATERIALS	1
POLYMERIZATION	3
FILM CASTING	3
2.2 FILM CHARACTERIZATION	3
2.3 DIRECT CURRENT MEASUREMENTS	4
2.4 TRANSIENT PHOTOCURRENT MEASUREMENTS	8
2.5 RADIATION INDUCED CONDUCTIVITY STUDIES	8
2.6 CONDUCTIVITY MEASUREMENTS ON RADIATION DAMAGED SAMPLES	8
2.7 ALTERNATING CURRENT MEASUREMENTS	8
2.8 PROCEDURES FOLLOWED IN ELECTRICAL MEASUREMENTS	9
3. RESULTS AND DISCUSSION	9
3.1 DARK CONDUCTIVITY AND PHOTOCONDUCTIVITY AS A FUNCTION OF VOLTAGE AND TEMPERATURE	9
3.2 SPECTRAL DEPENDENCE OF PHOTOCONDUCTIVITY	19
3.3 TRANSIENT PHOTOCONDUCTIVITY MEASUREMENTS	26
3.4 RADIATION INDUCED CONDUCTIVITY MEASUREMENTS	31
3.5 EFFECT OF HIGH DOSES OF 2 Mev ELECTRONS ON DARK CONDUCTIVITY AND PHOTOCONDUCTIVITY	34
3.6 DIELECTRIC CONSTANT AND LOSS AS A FUNCTION OF FREQUENCY AND TEMPERATURE	44
3.7 EFFECT OF HIGH DOSES OF 2 Mev ELECTRONS ON DIELECTRIC PROPERTIES	49
4. GENERAL CONCLUSIONS	49
REFERENCES	53

## FIGURES

	<u>Page</u>
1 STEPLADDER PYRRONES	2
2 WEIGHT LOSS OF PMDA-DAB AND BTDA-DAB FILMS ON HEATING UNDER NITROGEN	5
3 INFRA-RED SPECTRA OF PYRRONE FILMS	6
4 GENERAL ARRANGEMENT FOR DC DARK AND PHOTOCONDUCTIVITY STUDIES	7
5 CAPACITOR CELL WITH MOUNT	10
6 CURRENT-VOLTAGE CHARACTERISTICS (PMDA-DAB)	12
7 EFFECT OF CURING TIME ON RESISTIVITY OF PMDA-DAB	13
8 CURRENT-VOLTAGE CHARACTERISTICS (BTDA-DAB)	14
9 DARK CURRENT-VOLTAGE CHARACTERISTICS (PMDA-DAB)	15
10 DARK CURRENT-VOLTAGE CHARACTERISTICS (BTDA-DAB)	16
11 PHOTOCURRENT-VOLTAGE CHARACTERISTICS (PMDA-DAB)	17
12 PHOTOCURRENT-VOLTAGE CHARACTERISTICS (BTDA-DAB)	18
13 DARK CURRENT-TEMPERATURE RELATIONSHIP (PMDA-DAB)	20
14 DARK CURRENT-TEMPERATURE RELATIONSHIP (BTDA-DAB)	21
15 PHOTOCURRENT-TEMPERATURE RELATIONSHIP (PMDA-DAB)	22
16 PHOTOCURRENT-TEMPERATURE RELATIONSHIP (BTDA-DAB)	23
17 SPECTRAL DEPENDENCE OF PHOTOCURRENT (PMDA-DAB)	24
18 SPECTRAL DEPENDENCE OF PHOTOCURRENT (BTDA-DAB)	25
19 TIME DEPENDENCE OF PHOTOCURRENT AT DIFFERENT WAVELENGTHS (PMDA-DAB)	27
20 TYPICAL HOLE PHOTOCURRENT TRANSIENTS IN PYRRONE FILMS	28
21 TRANSIENT PHOTOCURRENT-VOLTAGE CHARACTERISTICS (BTDA-DAB)	29
22 TRANSIENT PHOTOCURRENT-VOLTAGE CHARACTERISTICS (PMDA-DAB)	30
23 RADIATION INDUCED CURRENT CHARACTERISTICS (PMDA-DAB)	33

FIGURES (CONTINUED)

	<u>Page</u>
24 RADIATION INDUCED CURRENT AS A FUNCTION OF RADIATION DOSE RATE FOR PMDA-DAB AND BTDA-DAB	37
25 CURRENT-VOLTAGE CHARACTERISTICS OF IRRADIATED PMDA-DAB SAMPLES (RADIATION DOSE = $1 \times 10^7$ RAD AT VARIOUS TEMPERATURES)	38
26 CURRENT-VOLTAGE CHARACTERISTICS OF IRRADIATED BTDA-DAB SAMPLES (RADIATION DOSE = $1 \times 10^7$ RAD AT VARIOUS TEMPERATURES)	39
27 CURRENT-VOLTAGE CHARACTERISTICS OF IRRADIATED PMDA-DAB AND BTDA-DAB SAMPLES (RADIATION DOSE = $1 \times 10^9$ RAD AT 20°C)	40
28 CURRENT-VOLTAGE CHARACTERISTICS OF IRRADIATED PMDA-DAB SAMPLES (RADIATION DOSE = $5 \times 10^9$ RAD AT VARIOUS TEMPERATURES)	41
29 CURRENT-VOLTAGE CHARACTERISTICS OF IRRADIATED BTDA-DAB SAMPLES (RADIATION DOSE = $5 \times 10^9$ RAD AT VARIOUS TEMPERATURES)	42
30 DIELECTRIC CONSTANT OF PMDA-DAB	45
31 DIELECTRIC CONSTANT OF BTDA-DAB	46
32 DIELECTRIC LOSS OF PMDA-DAB	47
33 DIELECTRIC LOSS OF BTDA-DAB	48

## TABLES

		<u>Page</u>
1	PREPOLYMER VISCOSITY AND ELEMENTAL ANALYSIS OF PMDA-DAB AND BTDA-DAB FILMS	4
2	CONDUCTION ACTIVATION ENERGIES FOR PYRRONES	19
3	TRANSIENT PHOTOCONDUCTION DATA ON PYRRONE SAMPLES	32
4	RADIATION INDUCED CURRENT DATA FOR PMDA-DAB	35
5	RADIATION INDUCED CURRENT DATA FOR BTDA-DAB	36
6	DARK AND PHOTOCURRENT LEVEL AT $10^3$ VOLT/CM FOR IRRADIATED PYRRONE SAMPLES	43
7	DIELECTRIC PROPERTIES OF IRRADIATED PMDA-DAB	50
8	DIELECTRIC PROPERTIES OF IRRADIATED BTDA-DAB	51

## ELECTRICAL CHARACTERISTICS OF PYRRONE POLYMERS

P. J. Reucroft, H. Scott, P. L. Kronick and F. L. Serafin

The Franklin Institute Research Laboratories

### 1. INTRODUCTION

< Polyimidazopyrrolone or Pyrrone polymers are a new class of aromatic-heterocyclic polymers which have outstanding thermal and radiolytic stability. > The effect of high energy radiation on mechanical strength, thermophysical properties and some electrical properties have been reported previously (ref. 1). < This report describes a more detailed determination of the alternating current (A.C.) and direct current (D.C.) electrical properties of two Pyrrone polymers and the effect of high energy radiation on these properties. > The polymers investigated are shown in Figure 1.

The technical assistance of P. Chairge, Research Chemist II, P. J. Hackett, Technical Associate II and J. B. Drew, Research Physicist I is gratefully acknowledged.

### 2. EXPERIMENTAL

#### 2.1 PREPARATION OF MATERIALS

Pyromellitic dianhydride (PMDA) (Princeton Chemical Research) was sublimed for 6 hours through two layers of fiberglass fabric onto a cold finger in a large laboratory sublimator at 200°/0.05 mm. Three similar runs yielded 69 g. of colorless sublimate melting at 286-287°. The yields were about 20-25%. Sublimation by entrainment in a stream of nitrogen was briefly investigated. Higher yields were obtained, but the sublimate had a slightly yellow color.

3,3',4,4'-Benzophenone tetracarboxylic acid dianhydride (BTDA) (Gulf Chemical Corp.) was similarly sublimed and resublimed at 255°/0.025 mm. Melting points of products ranged from 221-228°, apparently depending on exposure to moisture. The larger crystals which fell off the cold finger had the highest melting point when determined immediately following removal from sublimator. Crystalline powder which remained on the cold finger had a lower melting point, as did crushed larger crystals exposed to air a few minutes.

3,3'-Diaminobenzidine (DAB) (Burdick and Jackson Laboratories, Inc.) was recrystallized from a 2:1 mixture of water and acetonitrile after treatment with charcoal to yield a light tan powder, m.p. 176°, after vacuum drying for 2 days. A similar recrystallization from water yielded a slightly darker product, m.p. 174-175°. Recrystallized material was used in most of the exploratory polymerization studies. The films for electrical evaluation were prepared from DAB as received from NASA/Langley after vacuum drying one week at room temperature.

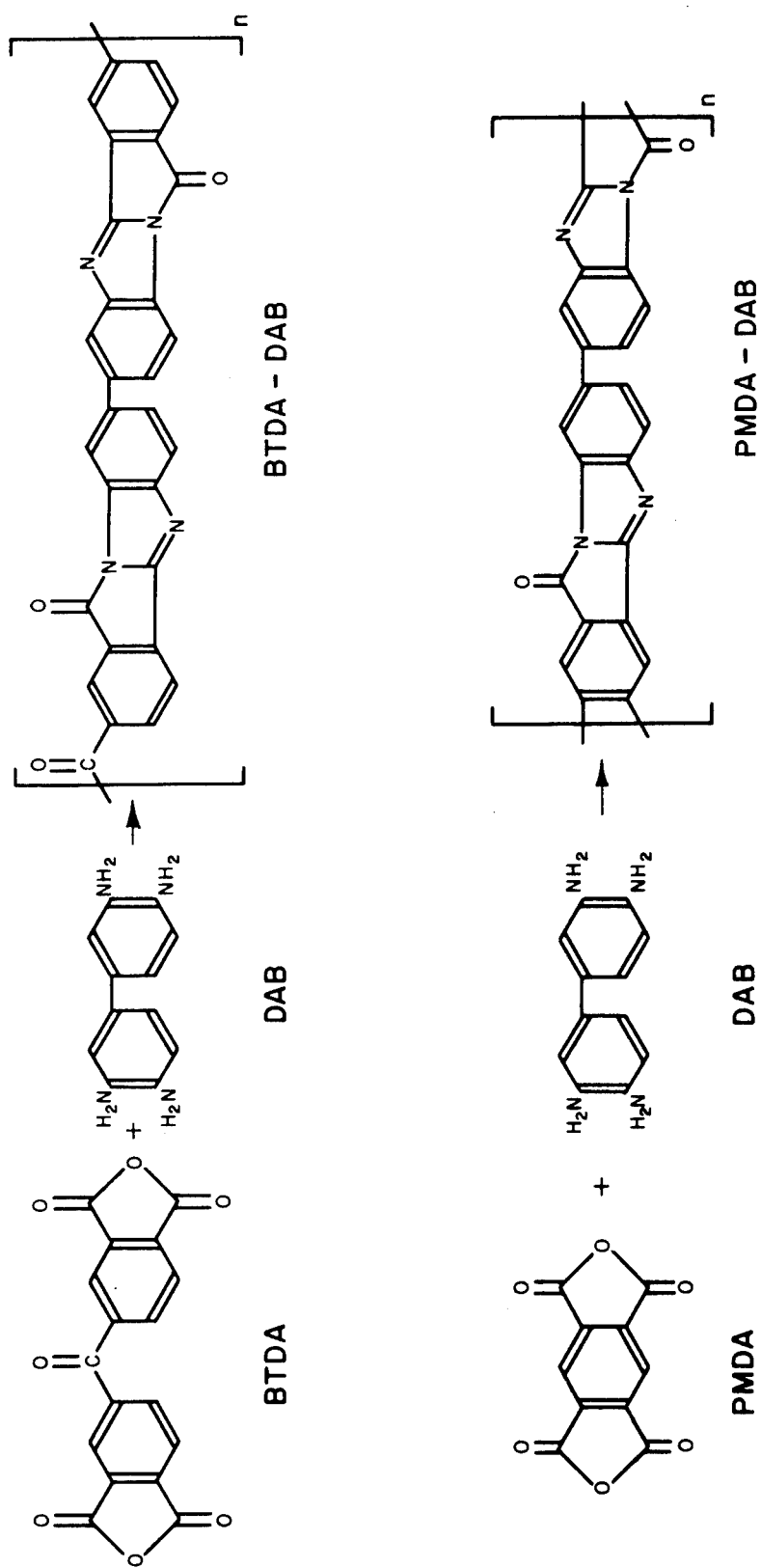


FIGURE 1 STEPLADDER PYRRONES.



Dimethylacetamide (E. I. du Pont de Nemours and Co., Inc.), 55 gal. drum quality, was supplied on special order in 5 gal. drum filled at plant under nitrogen. It was distilled from PMDA for use as solvent in preparation of films for electrical evaluation.

#### POLYMERIZATION

The procedures were similar to those described by investigators at NASA/Langley (ref. 1 and 2). The Pyrrone polymer of BTDA-DAB was prepared by adding 95 ml of a solution of 12.89 g. (0.04 m) of sublimed BTDA in 100 ml DMAC to a stirred, hot ( $\sim 60^{\circ}\text{C}$ ) solution of 8.56 g. (0.04 m) of DAB in 100 ml DMAC in a preheated high-speed blender under nitrogen. The blender was wrapped with heating tape. After 30 minutes of stirring, the remainder of the BTDA solution, 0.65 g. in 5 ml DMAC, was added dropwise. Stirring and heating were continued for one hour. Then the polymer dope was centrifuged. The supernatant was decanted off and stored under nitrogen in a dry ice chest.

The Pyrrone polymer of PMDA-DAB was prepared in a similar manner except that the vessel was not heated. Upon completion of addition of the PMDA solution, stirring at room temperature was continued for about one-half hour.

No excess anhydride was used in either polymer preparation.

#### FILM CASTING

Three solutions of each prepolymer in DMAC were mixed to yield a PMDA-DAB dope intrinsic viscosity  $[\eta] = 1.02 \text{ dl/g}$  and a BTDA-DAB dope of  $[\eta] = 1.70 \text{ dl/g}$ . Films were cast from these solutions with an adjustable-clearance film applicator set at 6.0 mils clearance on a Pyrex glass plate, 21.5" x 10" x 1/4" polished on one side to 10 bands. This was done in a laminar flow work station. After the films were cast, gentle heat was applied beneath the plates from two infrared heating elements. After one and one-half hours, the plate was placed in a forced air oven set at  $100^{\circ}\text{C}$ . The films were cured at  $100^{\circ}$  for three hours,  $200^{\circ}$  for two hours, and  $300^{\circ}$  for one hour. After this curing cycle, the films were stripped from the glass plate while it was submerged in a water bath to facilitate removal. The films were then cured for another 24 hours at  $300^{\circ}$ .

Film thickness ranged from 10-50 microns. The thickest films were used for the dielectric loss measurements. All films used in measurements were free of pinholes as determined electrically by the Hg drop method and by microscopic observation.

#### 2.2 FILM CHARACTERIZATION

The intrinsic viscosities of solutions of PMDA-DAB and BTDA-DAB prepolymers and elemental analyses of cast films after curing 1 hour at  $300^{\circ}$  are shown in Table 1. Thermogravimetric analyses are

TABLE 1

PREPOLYMER VISCOSITY<sup>a</sup> AND ELEMENTAL ANALYSIS<sup>b</sup> OF PMDA-DAB AND BTDA-DAB FILMS

	$[\eta]$	<u>C</u>	<u>H</u>	<u>N</u>
PMDA-DAB	1.02			
Calc. for $C_{22}H_8N_4O_2$		73.33	2.22	15.56
Found		69.28	3.44	15.58
BTDA-DAB	1.70			
Calc. for $C_{29}H_{12}N_4O_3$		75.00	2.59	12.07
Found		71.29	2.79	11.77

<sup>a</sup> Final intrinsic viscosity in dl/g of a blend of smaller prepolymer dopes prepared from equimolar amounts of the amine and anhydride.

<sup>b</sup> %. Average of duplicate determinations by Galbraith Laboratories.

shown in Figure 2\*. Infrared absorption spectra of these films are shown as solid curves in Figure 3. The spectra of films which were further cured at 300° for 24 hours are shown as dotted curves.

### 2.3 DIRECT CURRENT MEASUREMENTS

The experimental arrangement used for measuring D.C. dark current and photocurrent in polymer film samples is shown schematically in Figure 4. Polymer films measured ranged in thickness from 10-50 microns. The two measuring electrodes consisted of evaporated gold, 1 sq cm in area. The electrode upon which illumination was allowed to fall transmitted 10-40% of incident light in the wavelength region 200-700 mμ. A grounded guard ring electrode was evaporated around the perimeter of the dark electrode to eliminate surface conductivity.

Currents were measured at applied field strengths in the range  $10^2$ - $10^6$  volt/cm with a Cary Model 31/31V Vibrating reed electrometer. A Keithley Model 240 D.C. power supply was used to supply voltage to the sample. Photocurrents were measured with a positive D.C. voltage applied

---

\* The slight dips in the curves at low temperature are believed to be due to an instrumental error since there is no reason to expect a gain in weight.

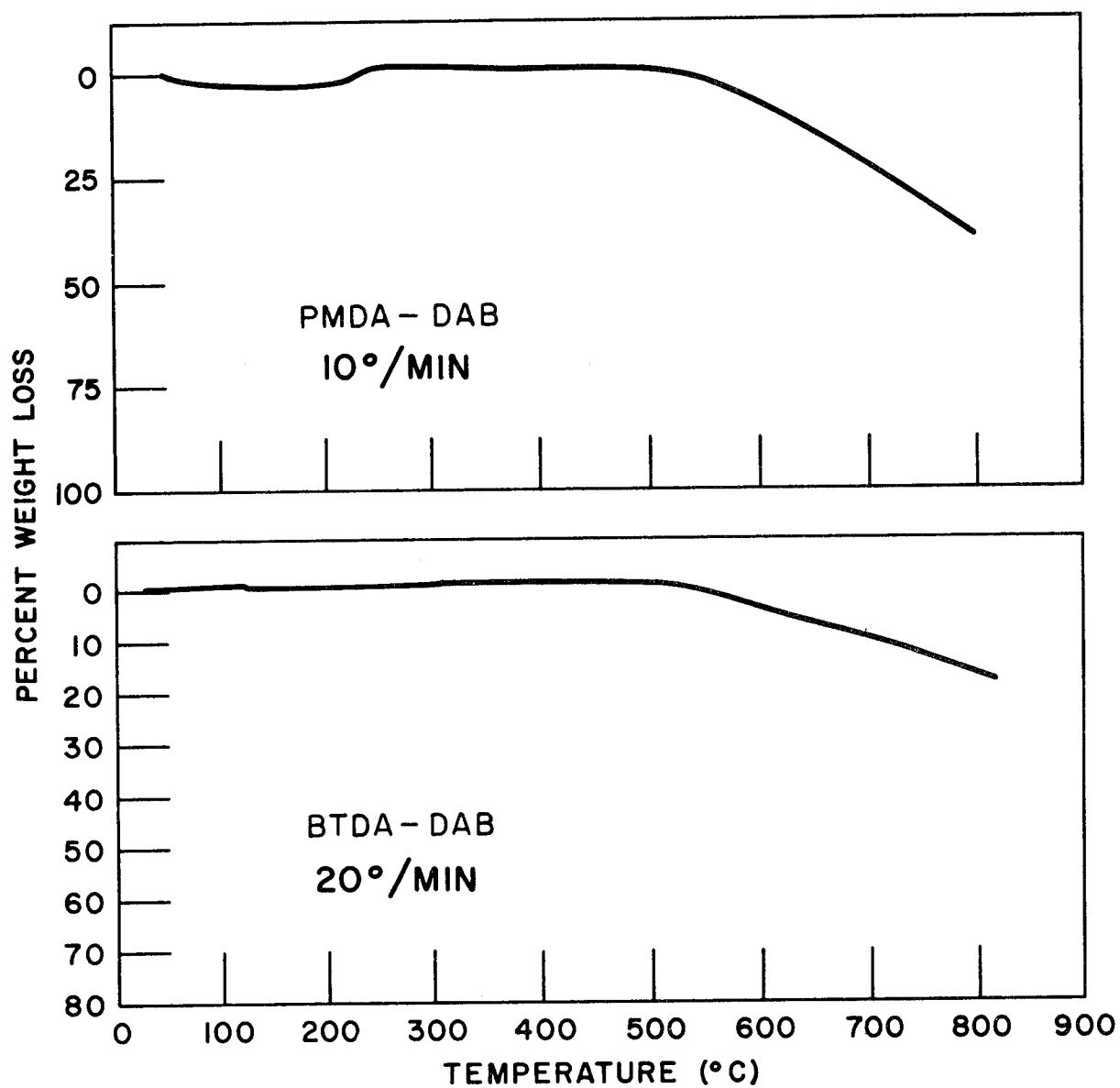


FIGURE 2 WEIGHT LOSS OF PMDA-DAB AND BTDA-DAB FILMS ON HEATING UNDER NITROGEN.

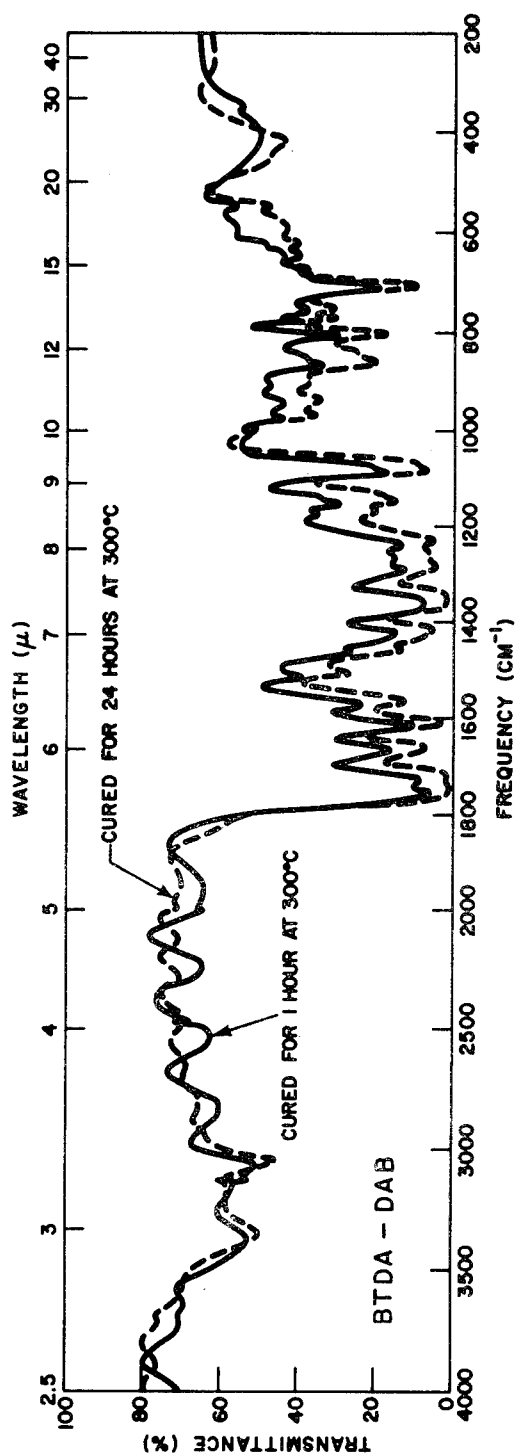
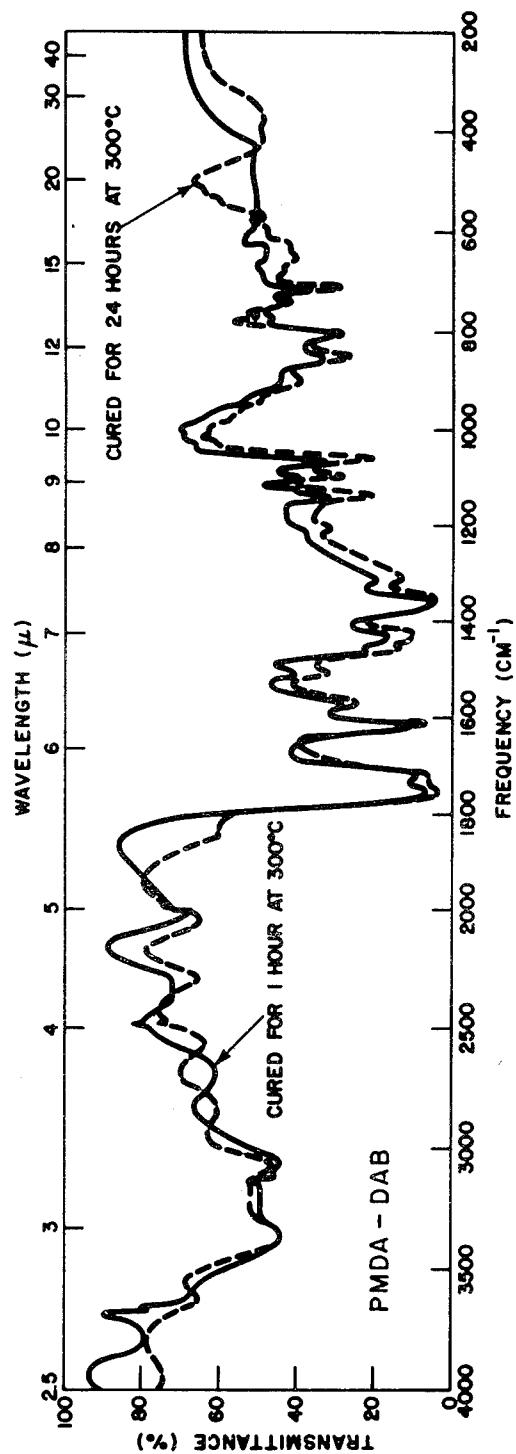


FIGURE 3 INFRARED SPECTRA OF PYRRONE FILMS.

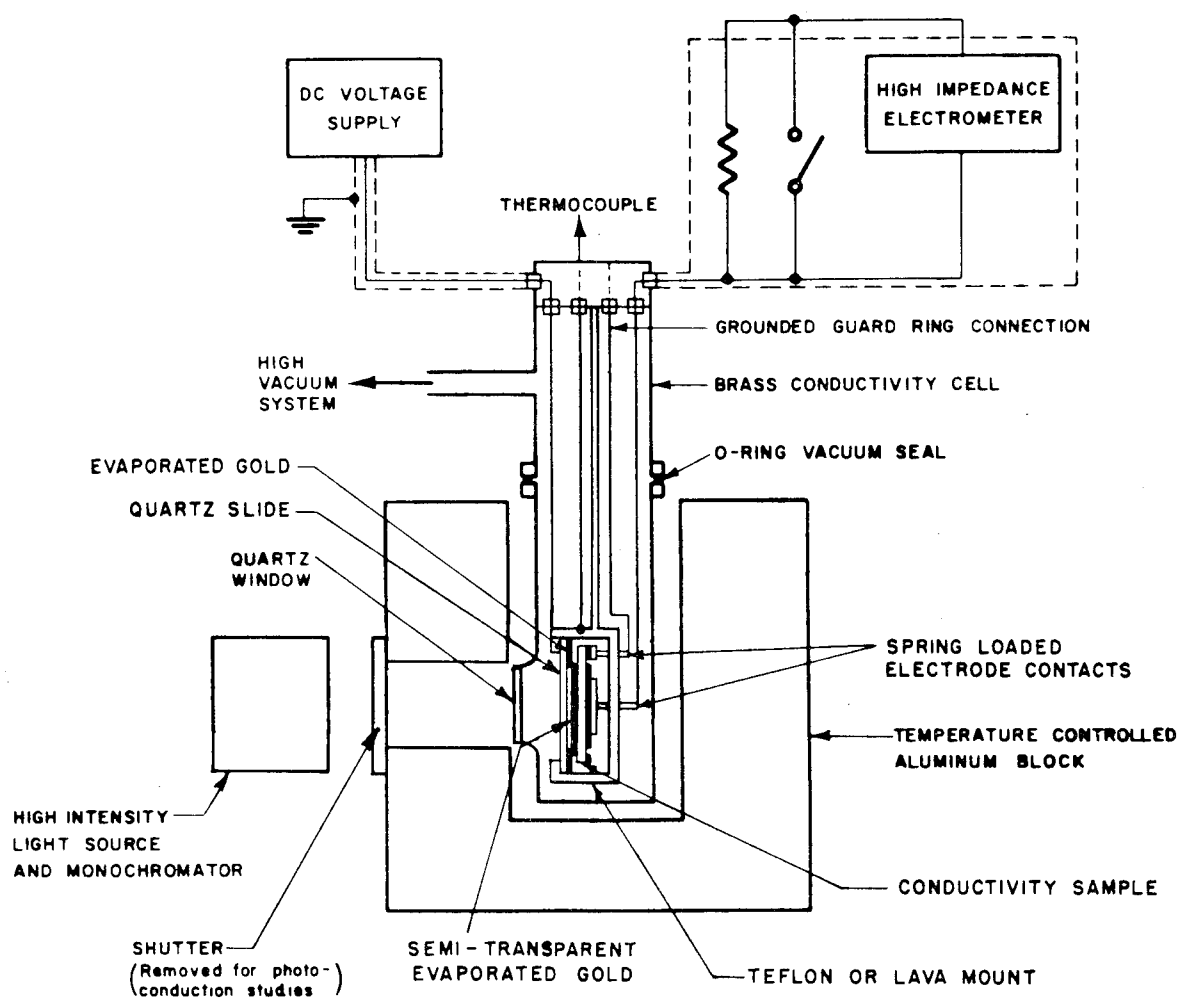


FIGURE 4 GENERAL ARRANGEMENT FOR DC DARK AND PHOTOCONDUCTIVITY STUDIES.

to the illuminated electrode.

A 1000 W Mercury lamp was used as a polychromatic light source. Monochromatic light was obtained from a Bausch and Lomb 150W Xenon Light Source in conjunction with Bausch and Lomb Monochromator gratings No. 33-86-01, No. 33-86-02 and No. 33-86-03.

#### 2.4 TRANSIENT PHOTOCURRENT MEASUREMENTS

Transient photoconductivity measurements were carried out using the experimental arrangement described previously (ref. 3). A General Radio Co. Strobotac, Type 1531-A, was used as a pulsed light source in these studies (flash duration 1 to 3 microseconds). All measurements were carried out with a positive D.C. voltage applied to the illuminated electrode.

#### 2.5 RADIATION INDUCED CONDUCTIVITY STUDIES

Radiation induced conductivity was determined using a 4000 Curie Gammabeam 150C gamma irradiation facility supplied by The Atomic Energy of Canada Limited. Radiation dose rates in the range 10 to 1000 rad/min were employed. The arrangement for measuring radiation induced conductivity was similar to that used in the dark and photocurrent investigations. Radiation was allowed to fall on the sample through a 20 mil aluminum window in the conductivity cell. The radiation dose was measured inside the cell at the sample location by means of thermoluminescent dosimetry. TLD-100 LiF thermoluminescent powder, supplied by Harshaw Chemical Co., was used in the calibration, the thermoluminescent output being monitored by means of a thermoluminescence dosimetry reader made available through courtesy of Stein Research Center, Jefferson Medical College Hospital.

#### 2.6 CONDUCTIVITY MEASUREMENTS ON RADIATION DAMAGED SAMPLES

Pyrrone film samples were irradiated at temperatures ranging from 20°C to 300°C with 2 Mev electrons for accumulated doses ranging from  $10^7$  rad to  $5 \times 10^9$  rad at the radiation facilities at Electronized Chemicals Corporation, Burlington, Massachusetts. The samples were maintained in vacuo at  $10^{-3}$  torr or less and at the specified temperature throughout the dose accumulation. After accumulating the radiation dose, samples were transferred from the irradiation chamber to glass containers under an ultra-pure grade argon atmosphere. The sealed containers were shipped to The Franklin Institute, the samples being maintained under an argon atmosphere until samples were removed for conductivity evaluation. Conductivity evaluation consisted of measuring the dark and photocurrent at applied fields in the range  $10^2$ - $10^6$  volt/cm as described in Section 2.3

#### 2.7 ALTERNATING CURRENT MEASUREMENTS

The dielectric constant and dissipation factor of polymer film samples was measured at temperatures of 20, 100, 200 and 300°C at

frequencies ranging from  $10^2$  to  $10^5$  Hz by means of a General Radio Type 1615A capacitance bridge used with a General Radio Type 1232-A tuned amplifier and null detector. The dielectric constant was calculated directly from the capacitance by means of the following relationship:

$$C = 8.84 \times 10^{-8} \frac{KA}{d}$$

where C = Capacitance in microfarads ( $\mu F$ )

K = Dielectric constant

A = Area in sq cm

d = Dielectric thickness in cm

The dissipation factor was read directly from the bridge. The cell arrangement is shown in Figure 5. From room temperature to  $150^\circ C$ , thermal control was achieved by a thermostatted oil bath. For higher temperatures, an electrically heated aluminum block similar to that illustrated in Figure 4 was utilized.

Samples irradiated with 2 Mev electrons for accumulated doses ranging from  $10^8$  rad to  $5 \times 10^9$  rad at temperatures ranging from  $20^\circ C$  to  $300^\circ C$  were measured in the same experimental arrangement. The dielectric constant and dissipation factor were measured for these samples at frequencies ranging from  $10^2$  to  $10^5$  Hz at  $20^\circ C$ .

## 2.8 PROCEDURES FOLLOWED IN ELECTRICAL MEASUREMENTS

(a) The majority of the conductivity measurements were carried out on film samples that were cured as follows:

At least three hours at  $100^\circ C$ ; at least two hours at  $200^\circ C$ ; at least 24 hours at  $300^\circ C$ .

(b) In initial stages of the program samples were evacuated for at least twenty-four hours at  $10^{-3}$  torr before electrical measurements were carried out. Evacuating overnight i.e. about 15-16 hours was later found to produce no significant differences in electrical characteristics measured. The latter procedure was thus more often followed since it allowed electrical data to be obtained more efficiently.

## 3. RESULTS AND DISCUSSION

### 3.1 DARK CONDUCTIVITY AND PHOTOCONDUCTIVITY AS A FUNCTION OF VOLTAGE AND TEMPERATURE

In measuring the dark conductivity and photoconductivity of PMDA-DAB and BTDA-DAB polymer films the following procedure was adopted:

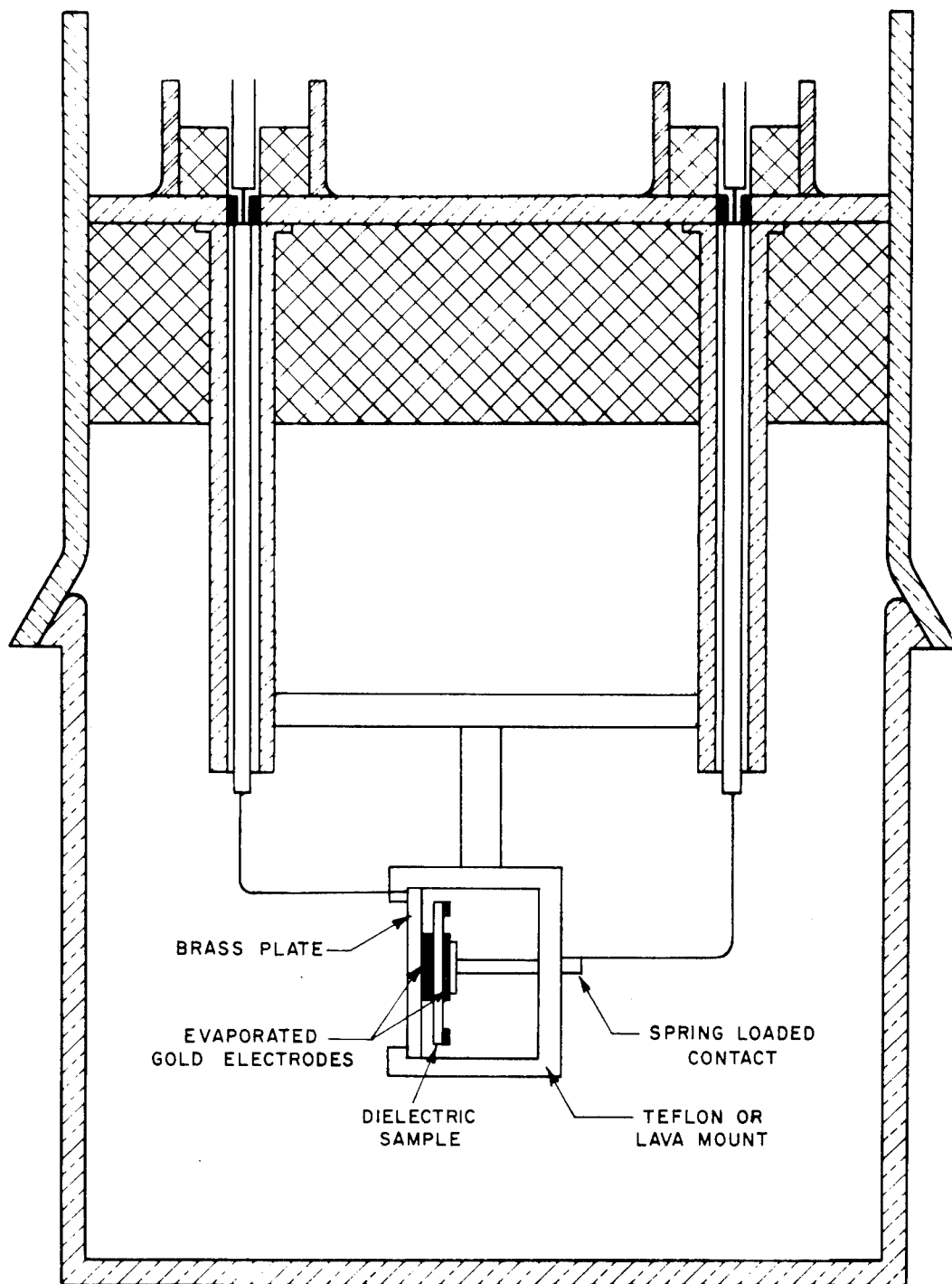


FIGURE 5 CAPACITOR CELL WITH MOUNT.



After evacuating the sample overnight at  $10^{-3}$  torr, voltage was applied to the sample and the current was read after approximately 0.5 to 1 hour. A slow decrease was still discernible at times longer than this, the current level decreasing by a factor of three to five after 24 hours. The current data shown in figures in the report refer to the current reading at 0.5 to 1 hour after applying voltage. Illumination was then allowed to fall on the sample producing an increase in current level. The photocurrent so produced leveled off in a few minutes with the polychromatic light source. Same variation in rise and decay time was found at different wavelengths when experiments with monochromatic light were carried out (See Section 3.2). On removing the illumination the current level fell quickly to the dark current level, approximately 90% of the photocurrent decaying in the first few minutes. The voltage was then increased and the procedure repeated. Increasing the voltage to breakdown allowed current-voltage characteristics to be compiled. Breakdown was taken as the onset of significant departure from a linear current-voltage characteristic, usually  $5 \times 10^5$  -  $10^6$  volt/cm. The sample was then equilibrated at successive temperatures in the region  $20^\circ\text{C}$  to  $300^\circ\text{C}$  and the procedure repeated. In this way current-voltage characteristics were obtained at several temperatures. Current as a function of temperature at constant applied strengths was derived from these plots.

The current characteristics with positive voltage applied to the illuminated electrode were virtually identical with those obtained with a negative voltage. The data reported were obtained with a positive voltage applied to the illuminated electrode.

Initial studies were carried out on PMDA-DAB samples cured for three hours at  $100^\circ\text{C}$ , two hours at  $200^\circ\text{C}$  and one hour at  $300^\circ\text{C}$ . The resistivity of these samples was in the range  $10^{11}$ - $10^{13}$  ohm-cm and photocurrent increases of about 50% above the dark current level were produced. On heating the sample for longer times at  $300^\circ\text{C}$  it was found that the dark resistivity increased by about 3 to 4 orders of magnitude. The photocurrent was now found to be at least an order of magnitude greater than the dark current. Figure 6 shows current-voltage characteristics obtained at room temperature for a short time and long time cured PMDA-DAB sample illustrating the above features. Measurement of resistivity as a function of curing time at  $300^\circ\text{C}$  showed that no further resistivity increase was found after 24 hours (Figure 7). Subsequently, all electrical measurements were carried out on samples cured for at least 24 hours at  $300^\circ\text{C}$ .

Dark current-voltage and photocurrent-voltage characteristics are shown in Figure 8 for BTDA-DAB illustrating the greater photocurrent-dark current ratio obtained for this polymer.

Dark current-voltage characteristics at several temperatures for PMDA-DAB and BTDA-DAB are shown in Figures 9 and 10 respectively. Photocurrent-voltage characteristics at several temperatures are shown in Figures 11 and 12.

The characteristics in Figures 6 and 8 show the photocurrent "as measured". In Figures 11 and 12 the photocurrent is corrected for dark current and refers to the current increase produced above the dark current level upon illumination.

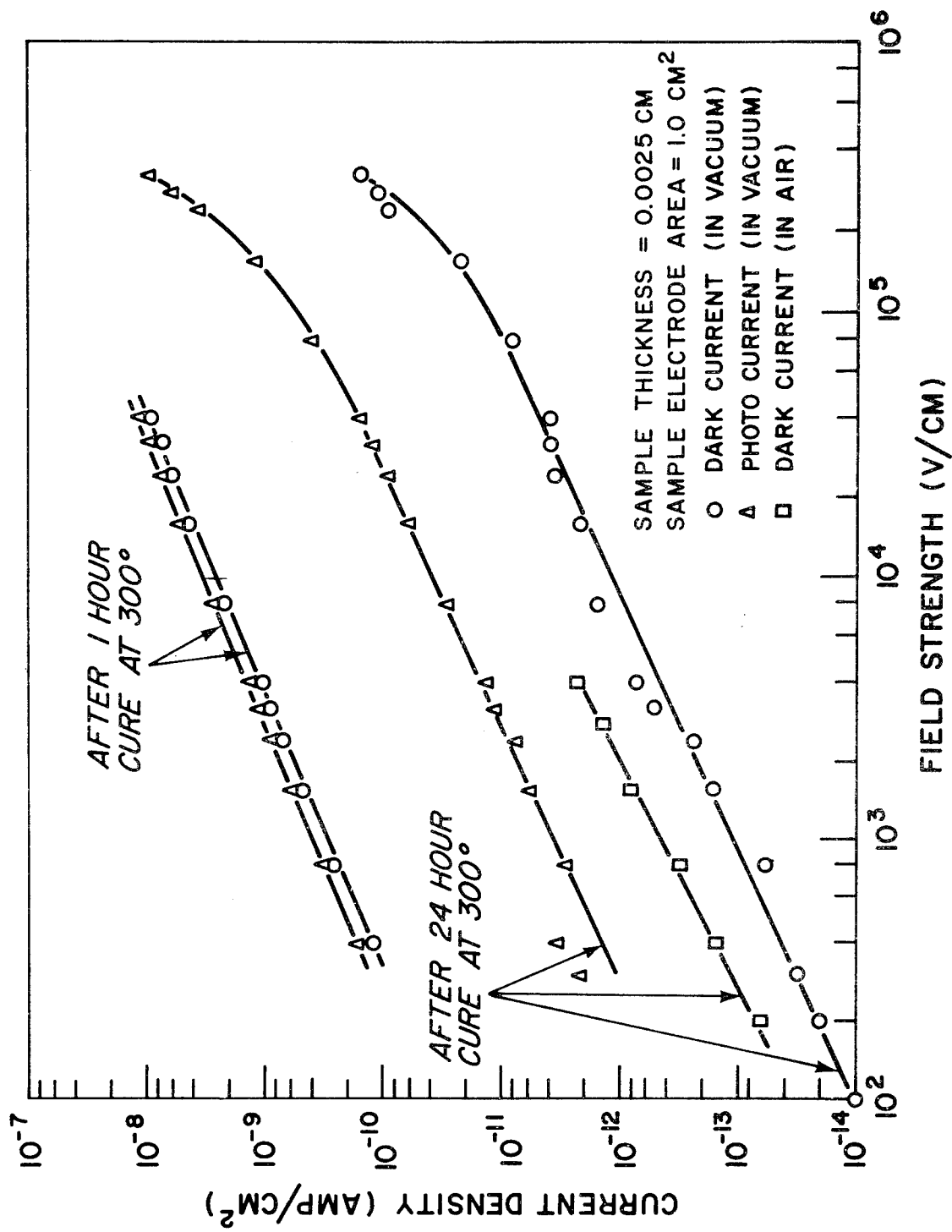


FIGURE 6 CURRENT-VOLTAGE CHARACTERISTICS (PMDA-DAB).

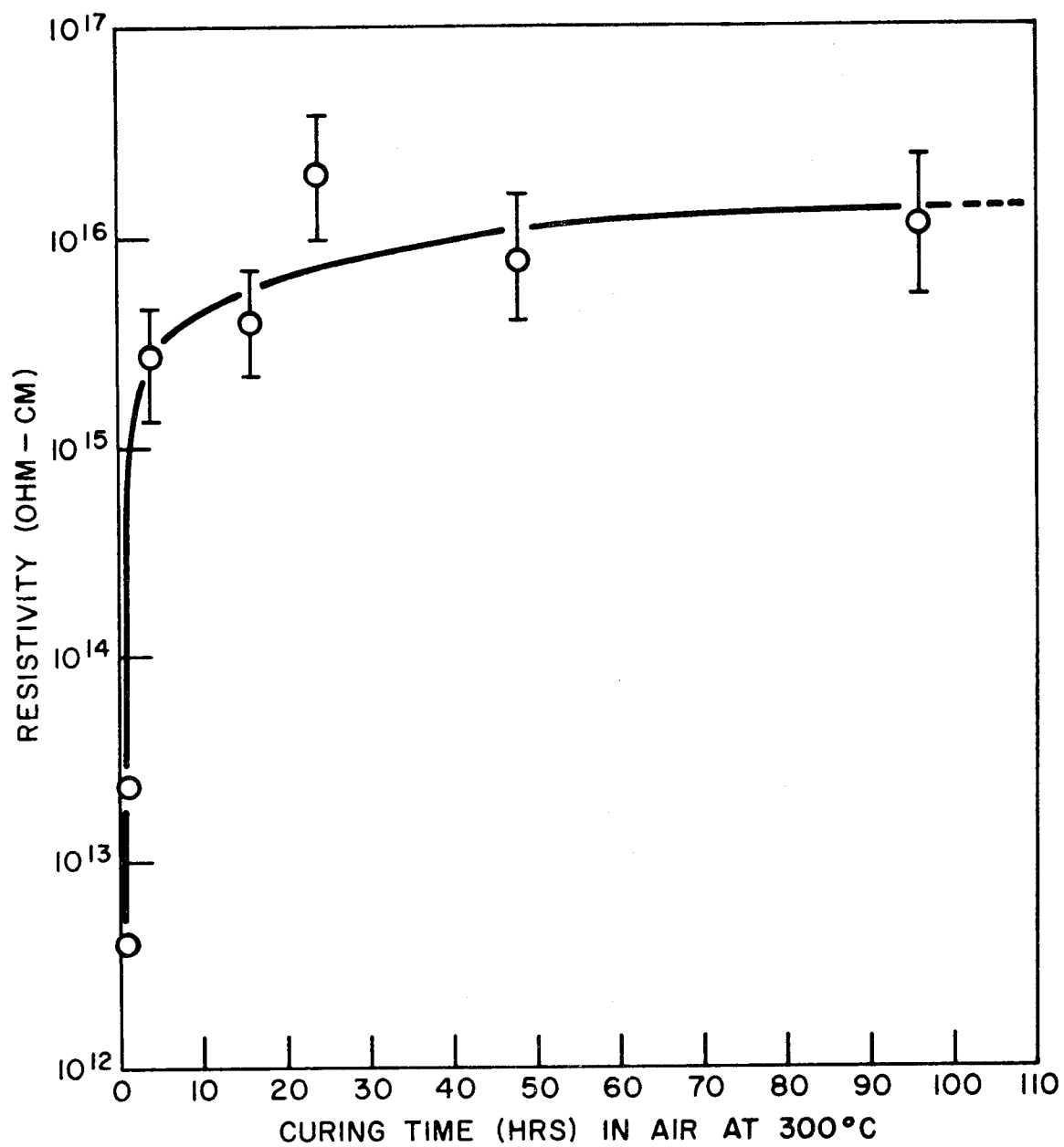


FIGURE 7 EFFECT OF CURING TIME ON RESISTIVITY OF PMDA-DAB.

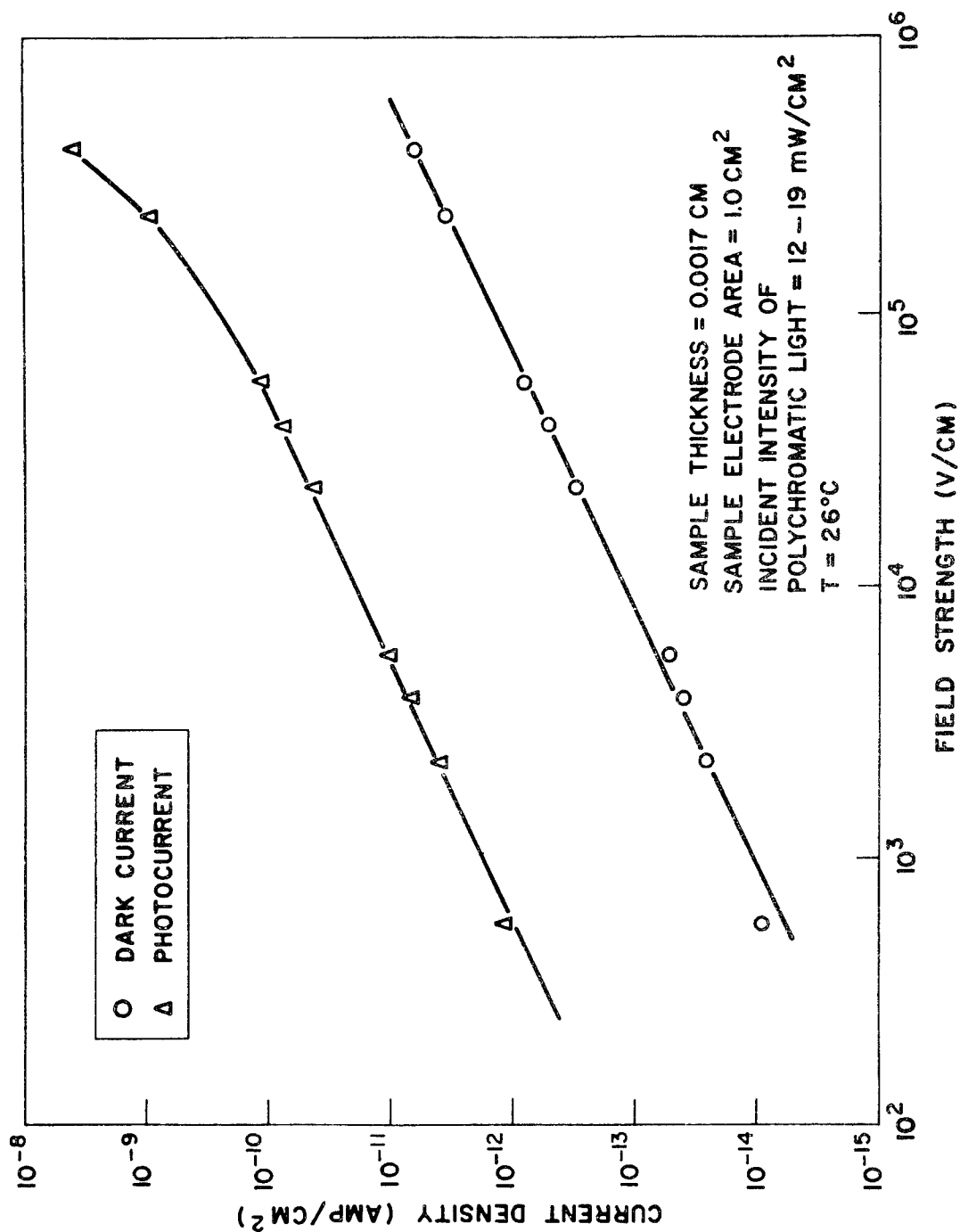


FIGURE 8 CURRENT-VOLTAGE CHARACTERISTICS (BTDA-DAB).

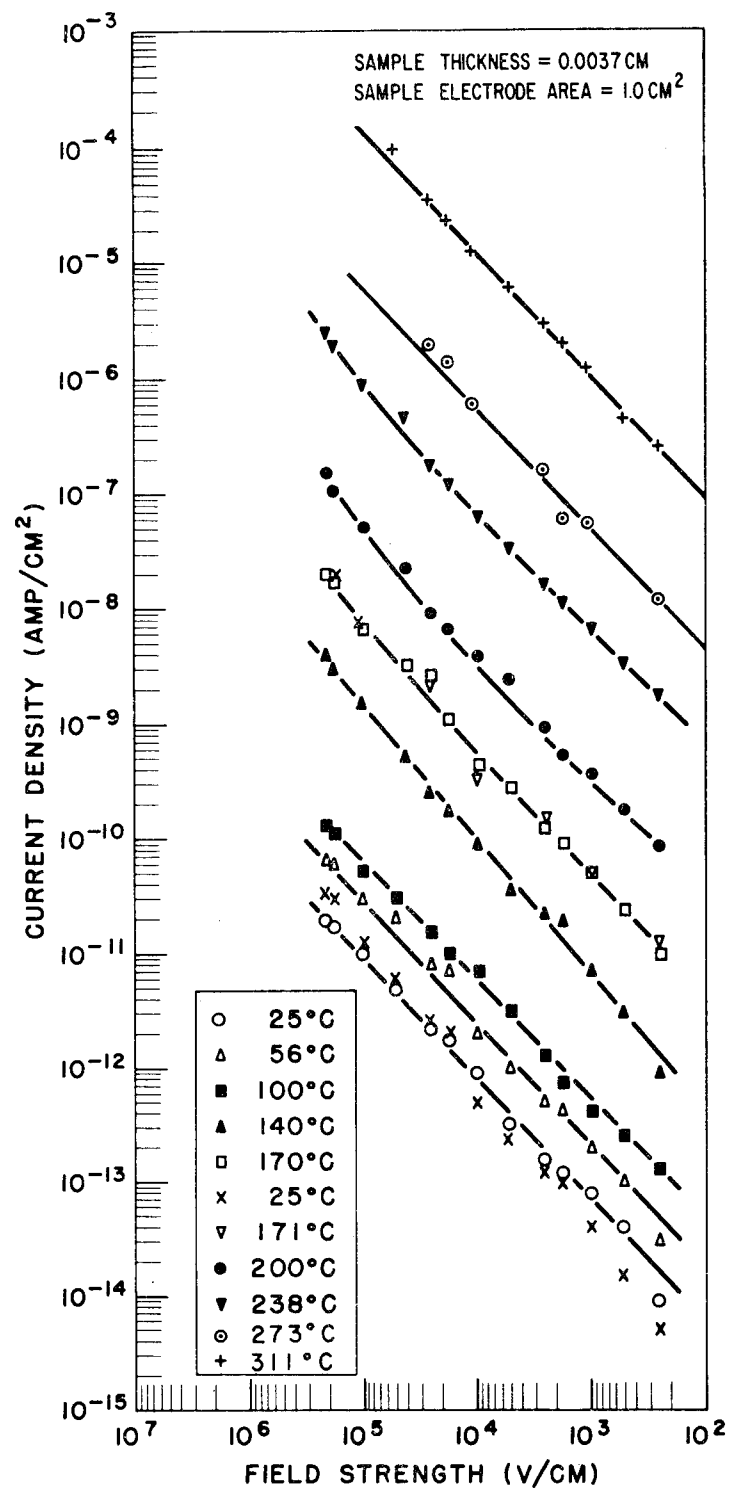


FIGURE 9 DARK CURRENT-VOLTAGE CHARACTERISTICS (PMDA-DAB).

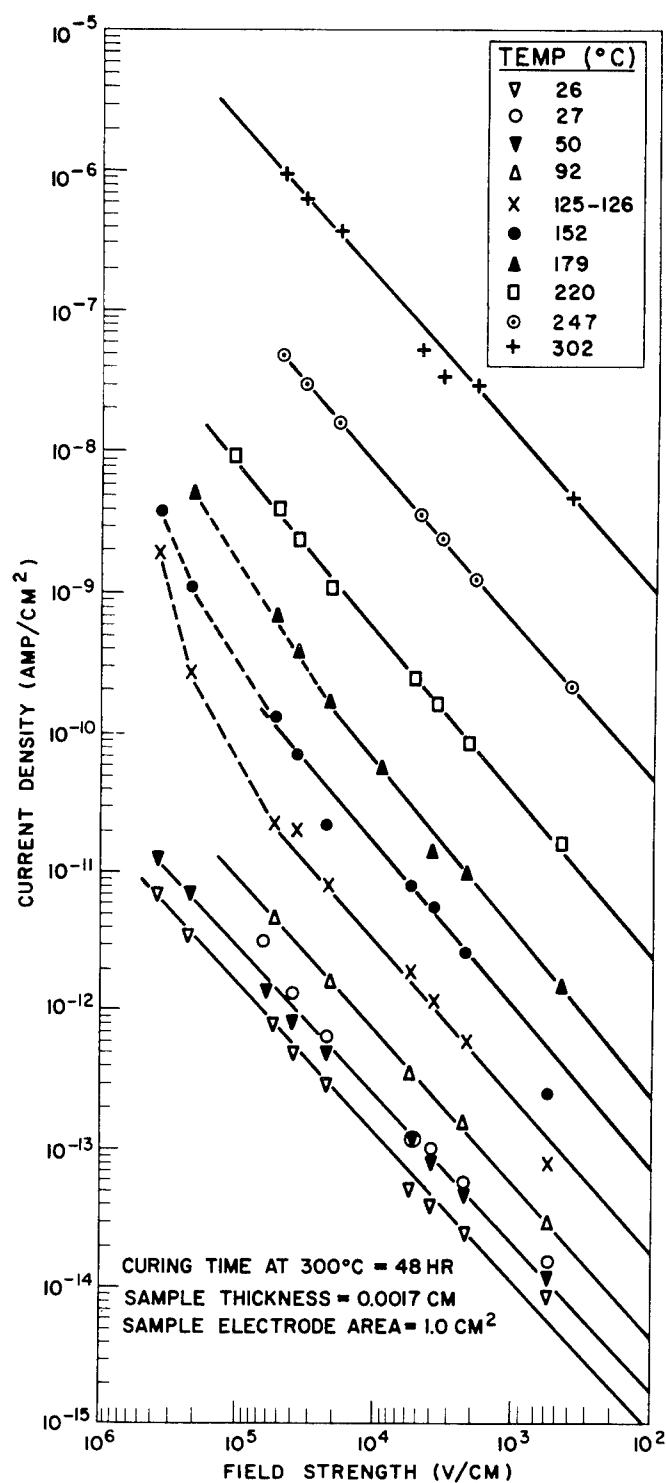


FIGURE 10 DARK CURRENT-VOLTAGE CHARACTERISTICS (BTDA-DAB).

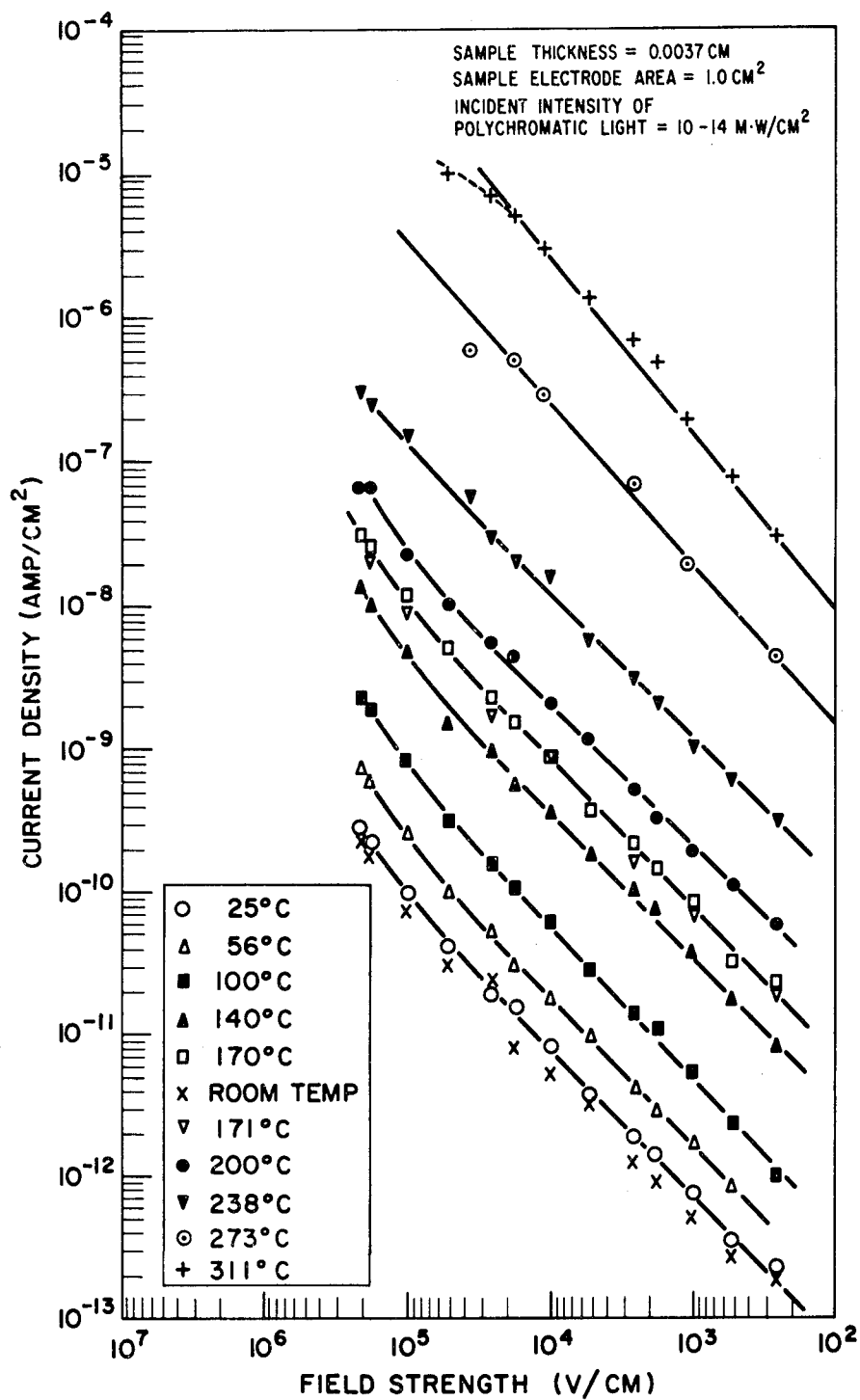


FIGURE 11 PHOTOCURRENT-VOLTAGE CHARACTERISTICS (PMDA-DAB).

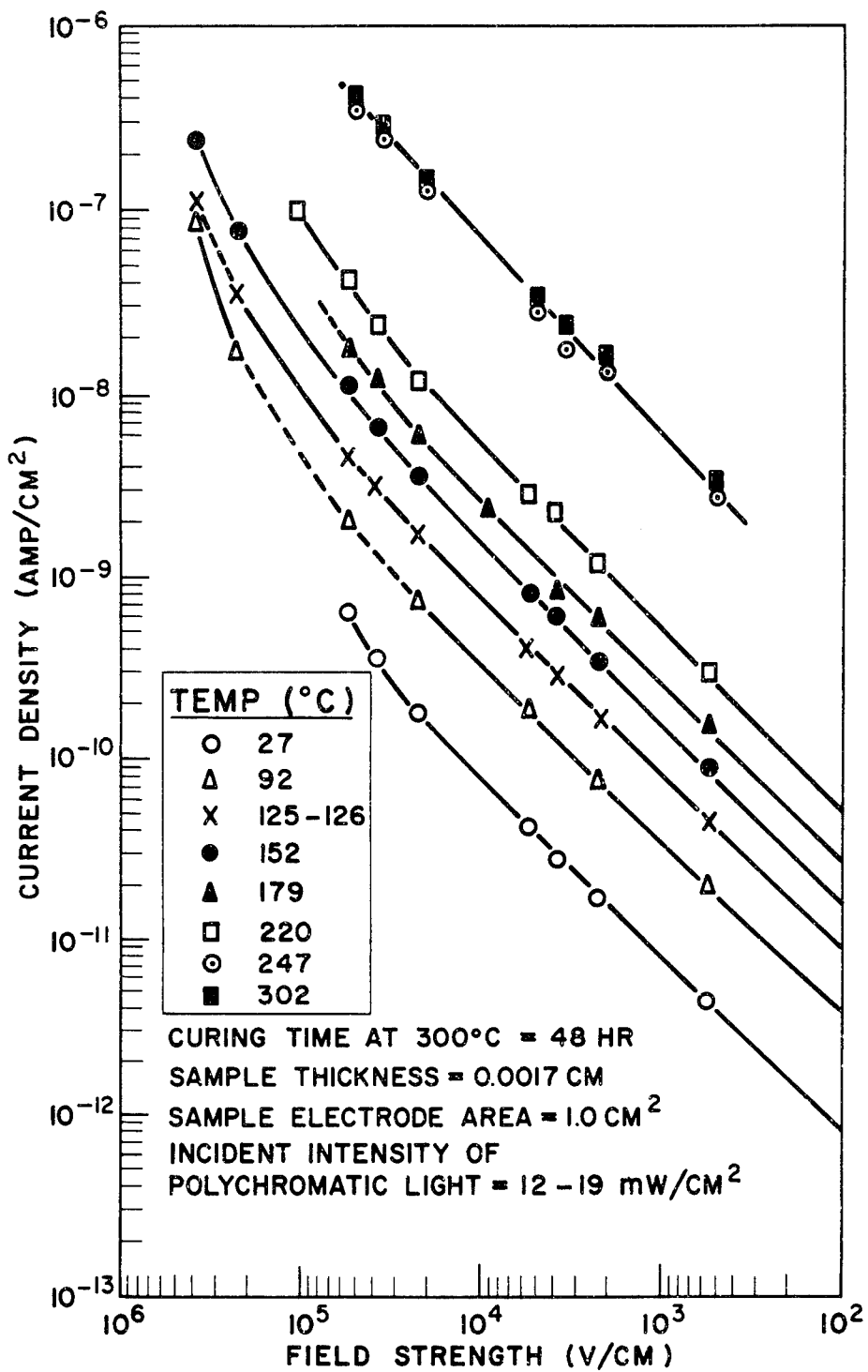


FIGURE 12 PHOTOCURRENT-VOLTAGE CHARACTERISTICS (BTDA-DAB).



Log (dark current) -  $\frac{1}{T^{\circ}K}$  plots are shown in Figures 13 and 14 for PMDA and BTDA-DAB respectively. Log (photocurrent) -  $\frac{1}{T^{\circ}K}$  plots are shown in Figures 15 and 16.

The main features of the dark conductivity and photoconductivity properties shown in Figures 6 to 16 can be summarized as follows:

1. Both Pyrrone polymers showed linear dark current and photocurrent-voltage characteristics with evaporated gold electrodes over an applied field strength range from  $10^2$  to  $10^6$  volt/cm.

2. BTDA-DAB polymer films are more photoconductive than PMDA-DAB films. The photocurrent-dark current ratio for BTDA-DAB ranged from 200-300, and for PMDA-DAB from 40-60 at  $20^{\circ}C$ .

3. Both dark current and photocurrent were reversible with temperature. After measuring the electrical characteristics at  $300^{\circ}C$  it was possible to return to lower temperatures and repeat the current-voltage characteristic previously obtained.

4. A non-linear relationship was found for the log (current) -  $\frac{1}{T^{\circ}K}$  plots implying more than one mechanism for charge carrier generation in the temperature range studied if the current is described by the relationship  $I = I_0 \exp - \frac{E}{kT}$ . The ranges of E values obtained in the temperature range investigated are summarized in Table 2 for the two polymers.

TABLE 2

CONDUCTION ACTIVATION ENERGIES FOR PYRRONES

(Field Strength  $10^4$  volt/cm)

<u>Sample</u>	<u>Dark Conduction Activation Energy (EV)</u>
BTDA-DAB	0.3 → 1.0 ( $25^{\circ}C \rightarrow 300^{\circ}C$ )
PMDA-DAB	0.24 → 1.1 ( $25^{\circ}C \rightarrow 300^{\circ}C$ )
<u>Sample</u>	<u>Photoconduction Activation Energy (EV)</u>
BTDA-DAB	0.2 → 0.95 ( $25^{\circ}C \rightarrow 300^{\circ}C$ )
PMDA-DAB	0.28 → 1.3 ( $25^{\circ}C \rightarrow 300^{\circ}C$ )

3.2 SPECTRAL DEPENDENCE OF PHOTOCONDUCTIVITY

The spectral dependence of photocurrent in the wavelength region 200-1300 mμ is shown in Figure 17 for PMDA-DAB and Figure 18 for BTDA-DAB. The photocurrent is corrected to a constant incident intensity

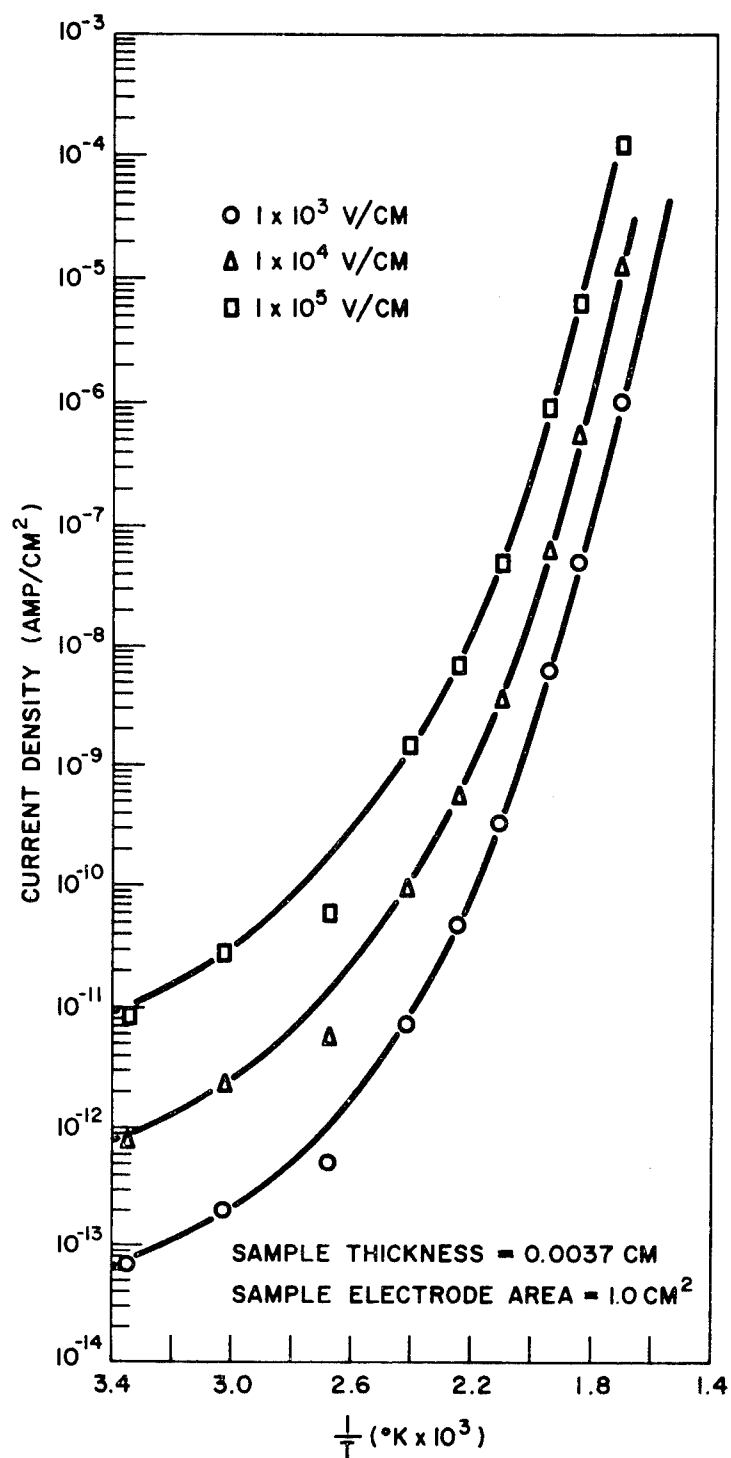


FIGURE 13 DARK CURRENT-TEMPERATURE RELATIONSHIP (PMDA-DAB).

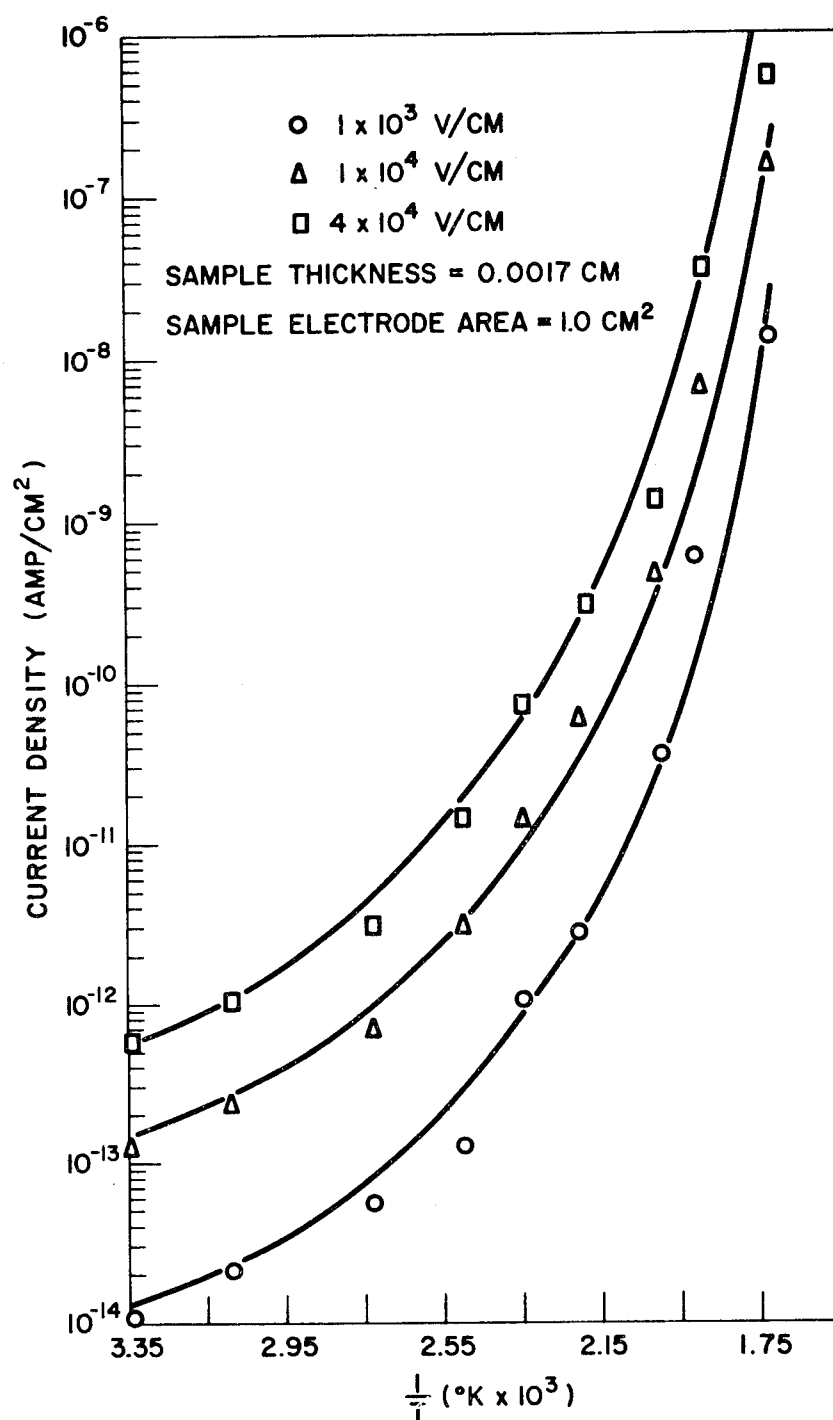


FIGURE 14 DARK CURRENT-TEMPERATURE RELATIONSHIP (BTDA-DAB).

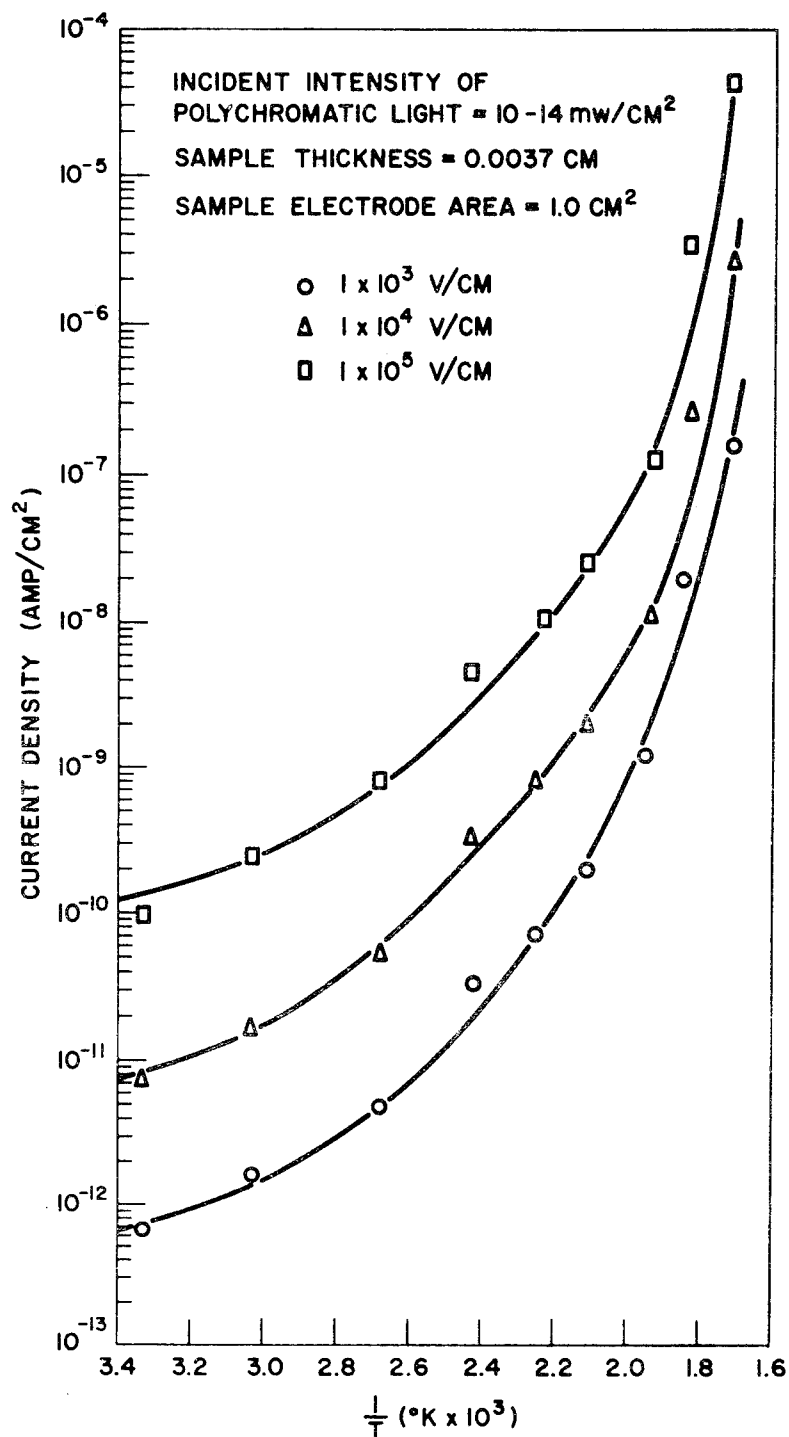


FIGURE 15 PHOTOCURRENT-TEMPERATURE RELATIONSHIP (PMDA-DAB).

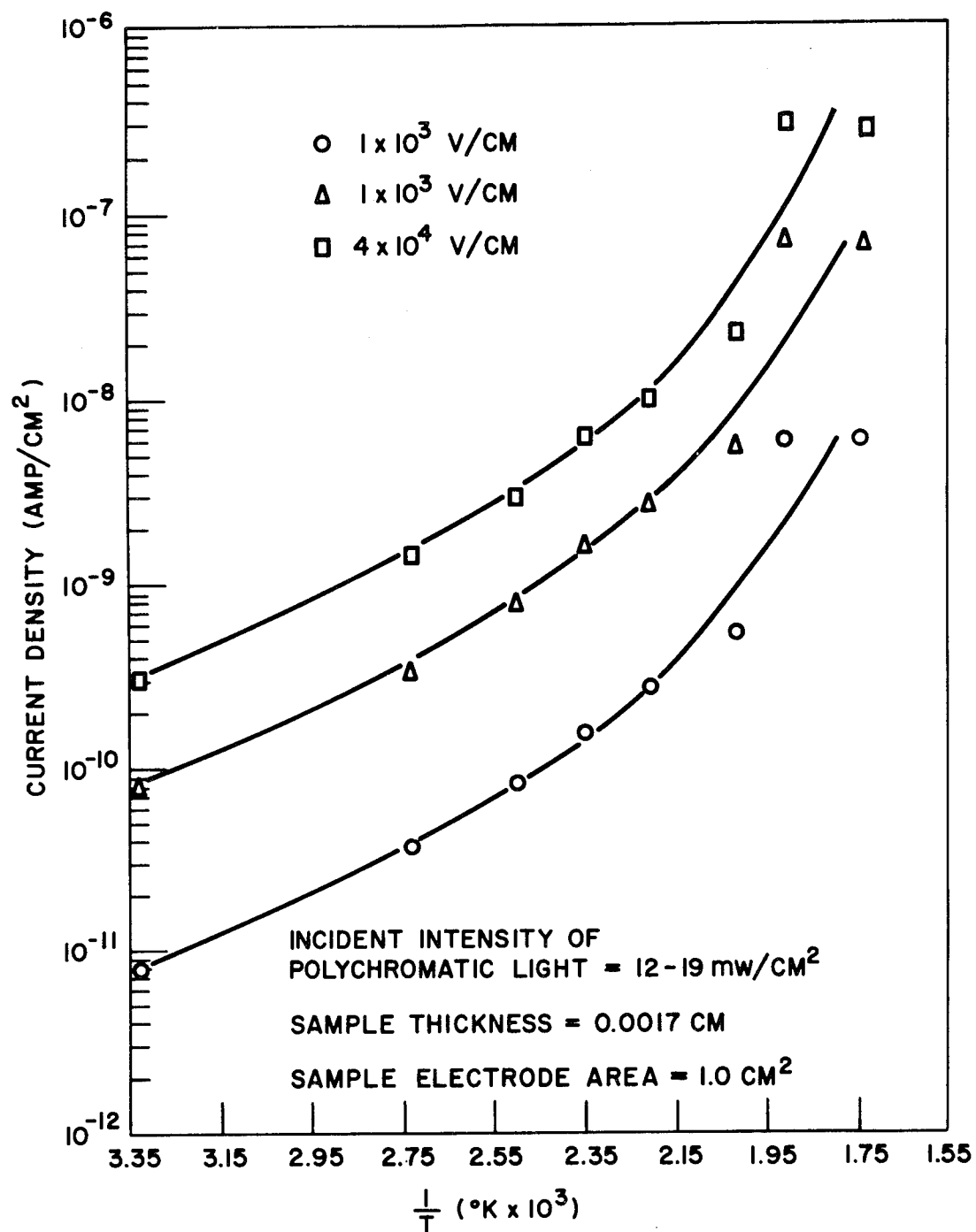


FIGURE 16 PHOTOCURRENT-TEMPERATURE RELATIONSHIP (BTDA-DAB).

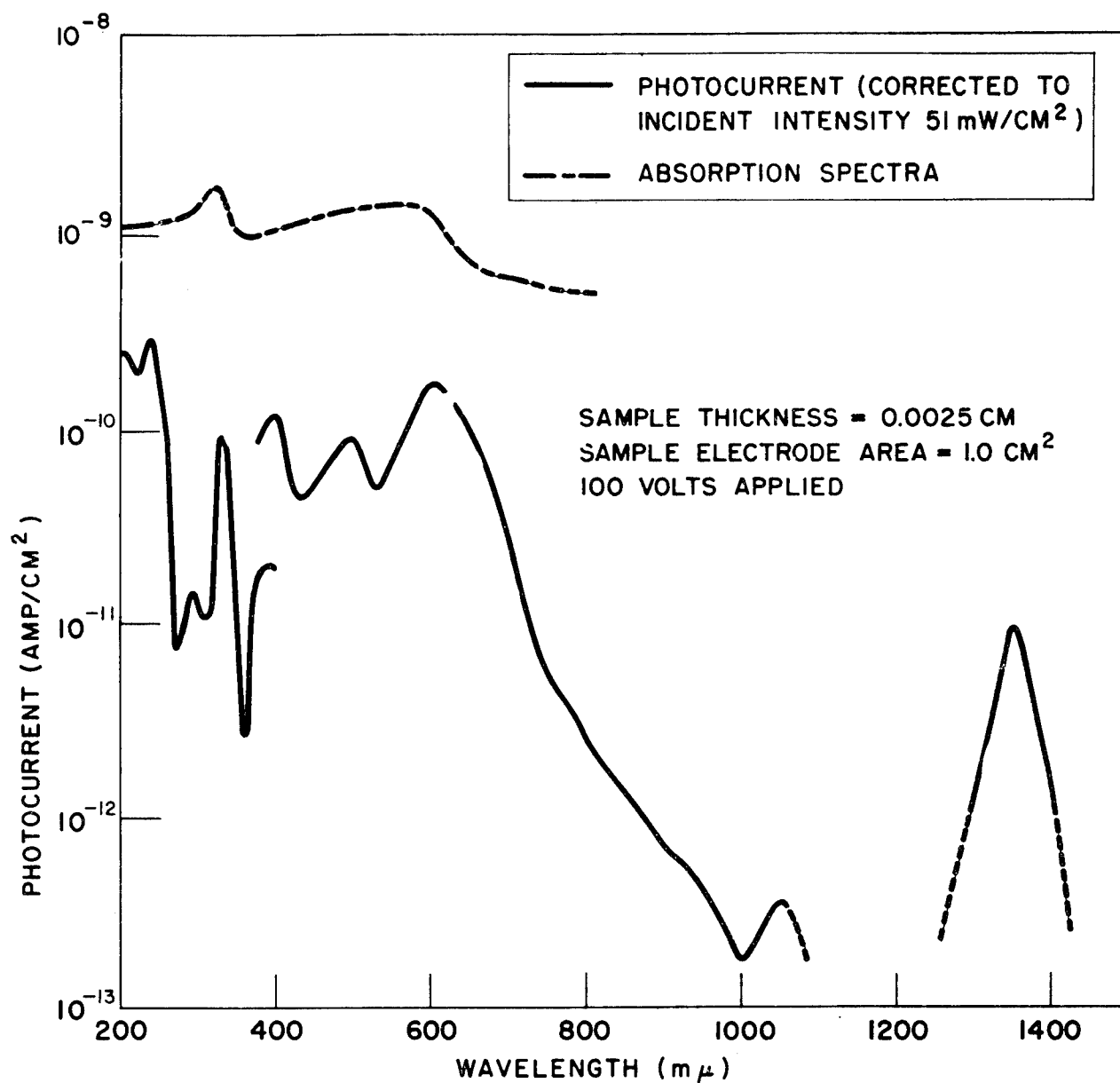


FIGURE 17 SPECTRAL DEPENDENCE OF PHOTOCURRENT (PMDA-DAB).

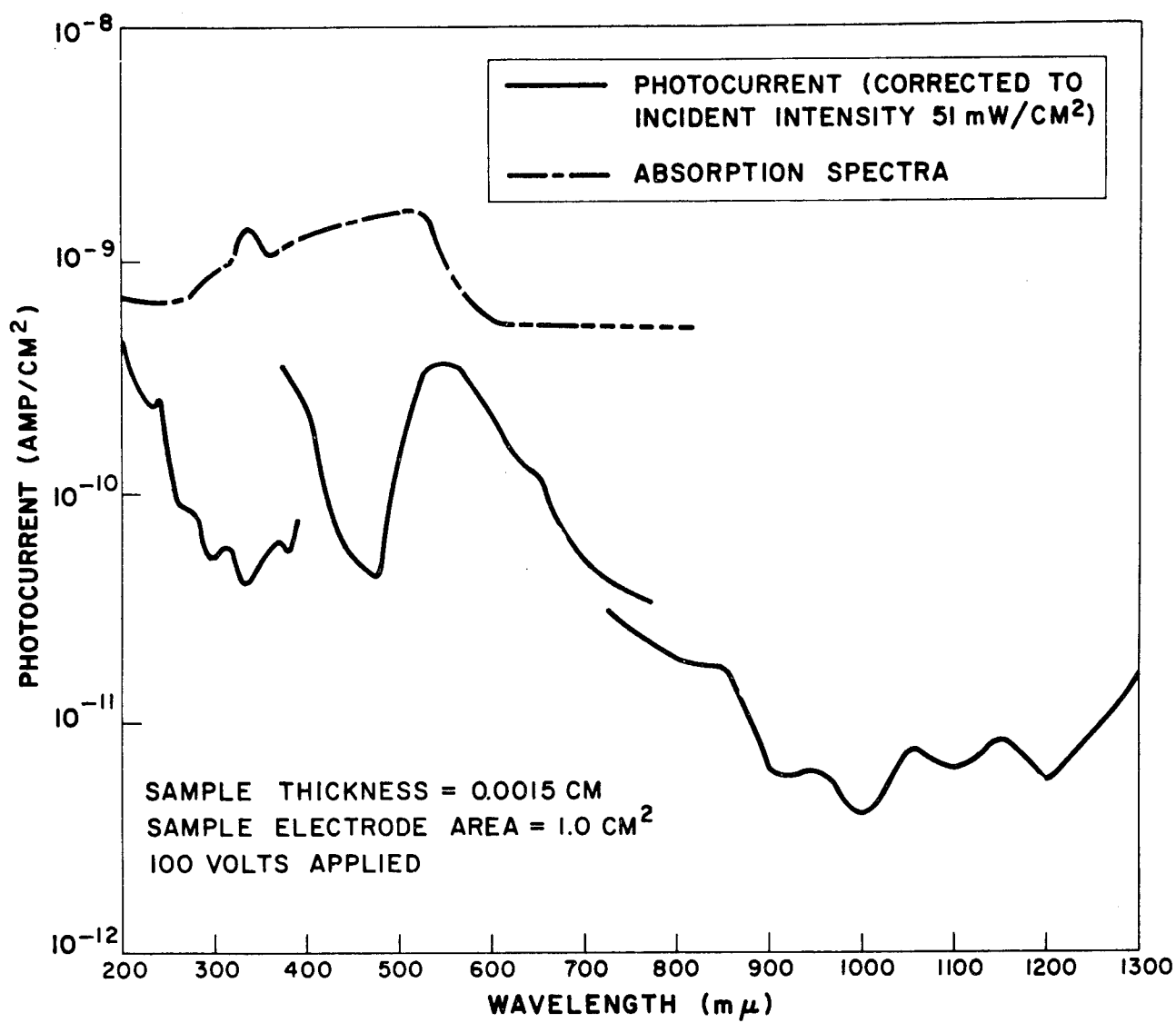


FIGURE 18 SPECTRAL DEPENDENCE OF PHOTOCURRENT (BTDA-DAB).

of monochromatic light. The optical spectra are also shown in Figures 17 and 18 for comparison. In general the main features of the optical spectra were found in the photocurrent spectra, the peak in the photocurrent spectra occurring 35 mμ to the red of that in the optical spectrum. The optical spectrum was obtained by means of a diffuse reflection spectroscopic technique, the intensity of light reflected from the sample being compared to a standard reflecting surface i.e. MgO. Transmission measurements yielded absorption edge data that were consistent with the reflection spectra.

Maximum photoefficiency for carrier generation was found in the visible and U.V. regions, the photocurrent peak occurring at 610 mμ for PMDA-DAB and 550 mμ for BTDA-DAB. The photoefficiency tailed off into the I.R. region, measurable effects being obtained at wavelengths as long as 1400 mμ.

Attempts to sensitize the BTDA-DAB polymer by adding dyes such as leuco-malachite green (48% and 16%) and cryptocyanine (9%) were not successful. The general spectral distribution of photocurrent was the same as for the undoped polymer, with the photocurrent depressed in two cases out of three. No new spectral regions of photoresponse were added to the overall photocurrent spectrum. The lack of sensitizing effect of dyes is most likely due to decomposition of the dye at the high temperature employed in curing the polymer films.

The rise and decay time of photocurrent was found to be influenced by wavelength of exciting light. The response time to reach peak photocurrent was about 60-100 secs in most regions of the spectrum. Six to seven minutes was required to reach maximum response at wavelengths in the region of the peak in the photocurrent spectrum. Figure 19 illustrates the rise and decay characteristics at several wavelengths for PMDA-DAB.

### 3.3 TRANSIENT PHOTOCONDUCTIVITY MEASUREMENTS

Transient photoconductivity studies were carried out to explore the feasibility of determining charge carrier mobility by the drift mobility technique (ref. 4). In this method a short lived (1-2 μ second) pulse of light is allowed to fall on the sample through a semitransparent electrode, generating a packet of carriers which then drift through the crystal under the influence of an applied field. The drift time of the carrier across the sample from electrode to electrode can be determined from the shape of the resulting transient photocurrent pulse recorded on an oscilloscope. The time of arrival is signified by the appearance of a "cusp" in the photocurrent transient. The mobility can be obtained from the drift time if the voltage applied to the sample and the sample thickness are known. If severe trapping of charge carriers occurs, however, a rapid decay of the photocurrent transient is observed which does not allow the drift time to be observed. In the case of Pyrrone samples this type of transient photocurrent signal was obtained in all samples investigated. Typically a peak signal was obtained in a few microseconds followed by a rapid decay. Typical transient photocurrent pulses for positive holes are shown in Figure 20. Transient photocurrent signals were obtained with peak values ranging from  $10^{-9}$  amp/cm<sup>2</sup> to  $10^{-7}$  amp/cm<sup>2</sup>. Transient photocurrent peaks are plotted as a function of applied voltage in Figures 21 and 22 for BTDA-DAB and PMDA-DAB samples respectively. A linear



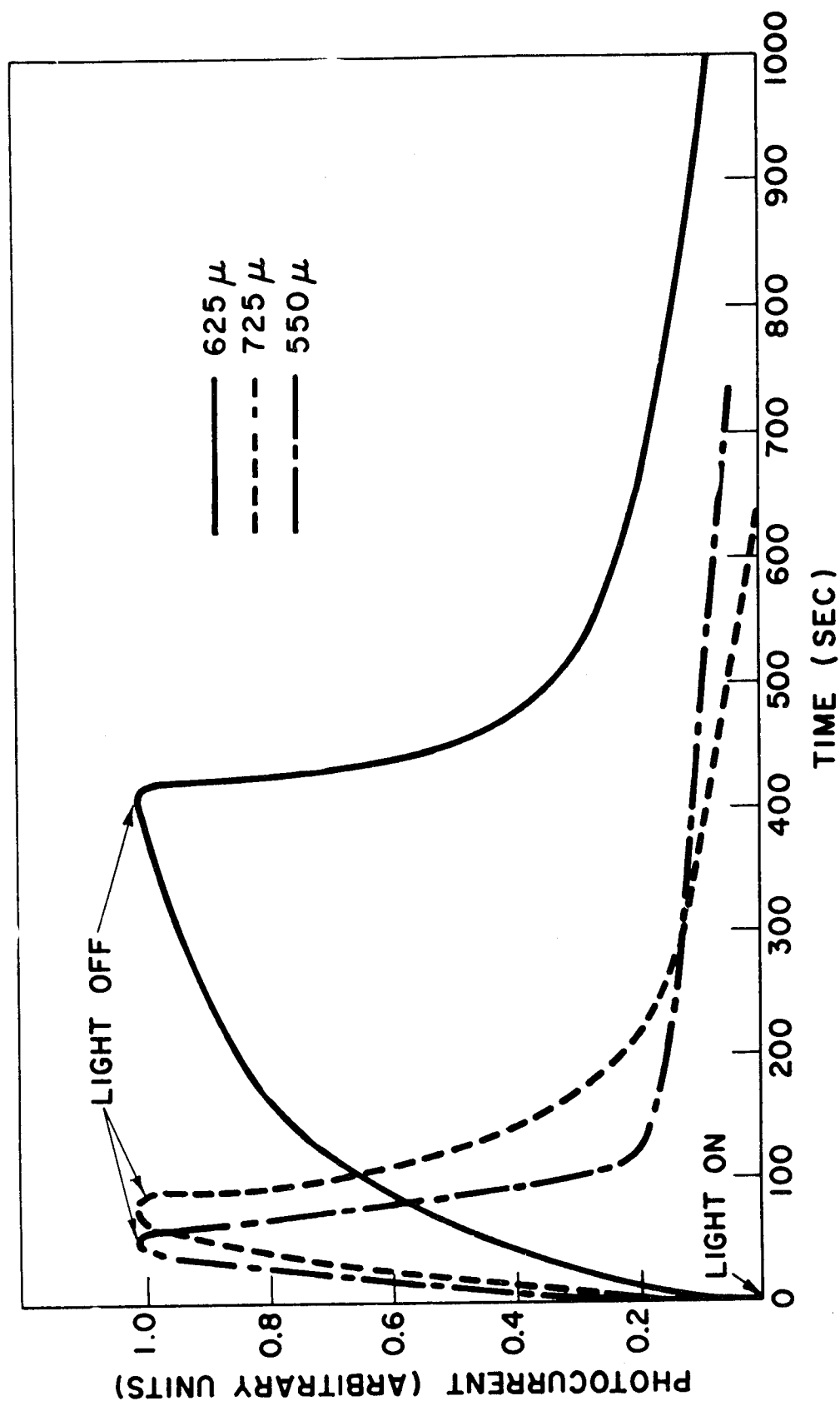
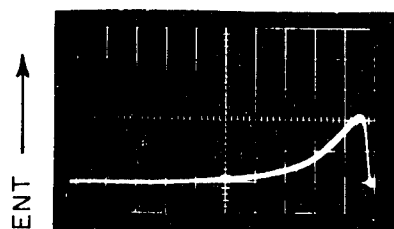


FIGURE 19 TIME DEPENDENCE OF PHOTOCURRENT AT DIFFERENT WAVELENGTHS (PMDA-DAB).

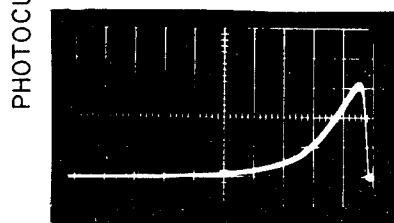
BTDA - DAB (Film Thickness  $1.8 \times 10^{-3}$  cm)



Current:  $1 \times 10^{-8}$  amp/large div.

Time: 50  $\mu$ sec/large div.

Applied Voltage: +500 V

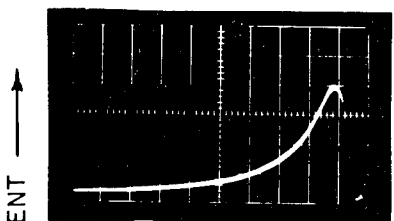


Current:  $1 \times 10^{-8}$  amp/large div.

Time: 50  $\mu$ sec/large div.

Applied Voltage: +600 V

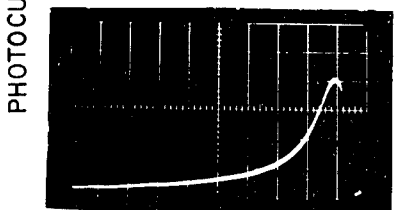
PMDA - DAB (Film Thickness  $3.5 \times 10^{-3}$  cm)



Current:  $4 \times 10^{-9}$  amp/large div.

Time: 10  $\mu$ sec/large div.

Applied Voltage: +500 V



Current:  $4 \times 10^{-9}$  amp/large div.

Time: 10  $\mu$ sec/large div.

Applied Voltage: +600 V

FIGURE 20 TYPICAL HOLE PHOTOCURRENT TRANSIENTS IN PYRRONE FILMS.

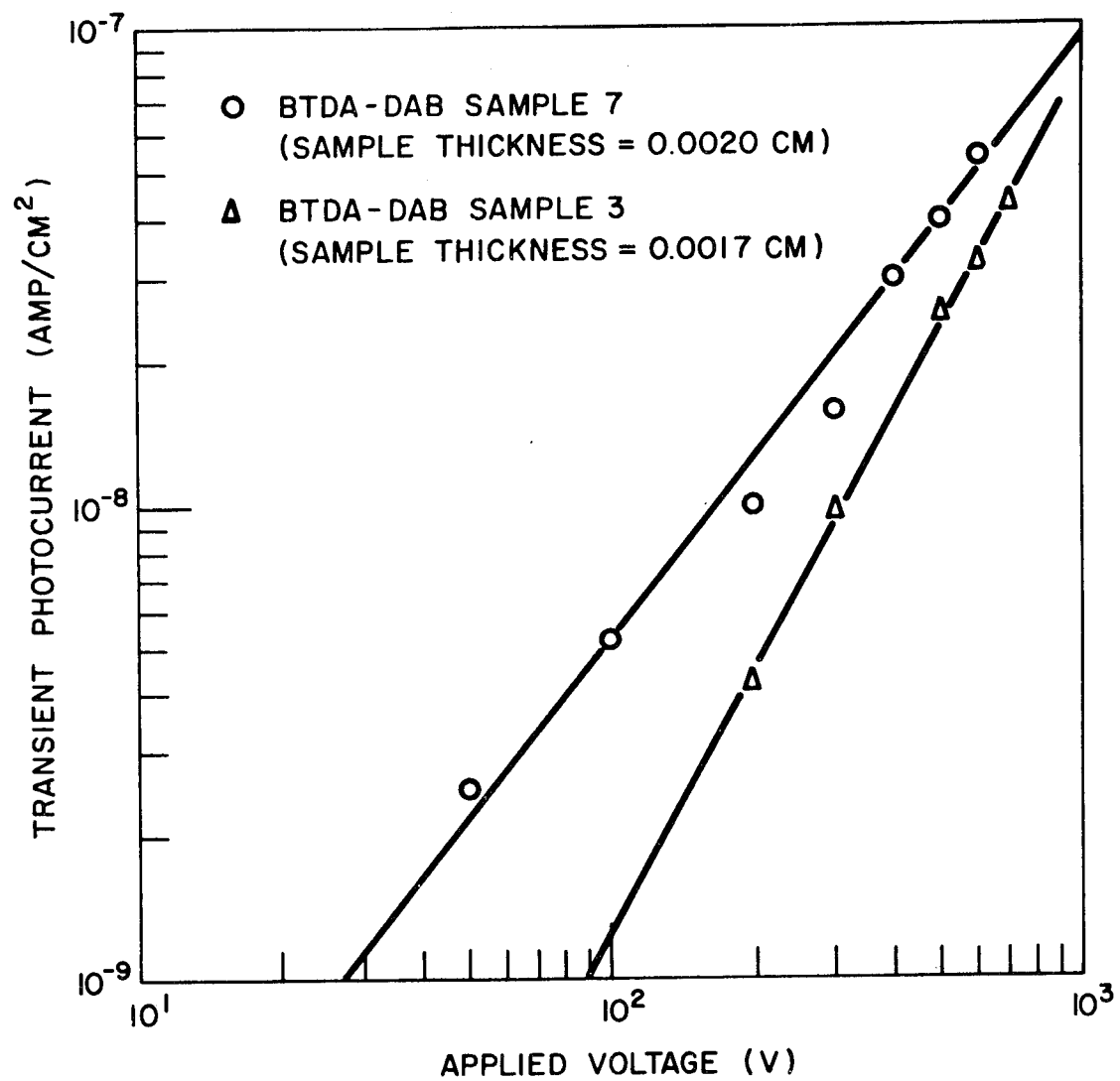


FIGURE 21 TRANSIENT PHOTOCURRENT-VOLTAGE CHARACTERISTICS (BTDA-DAB).

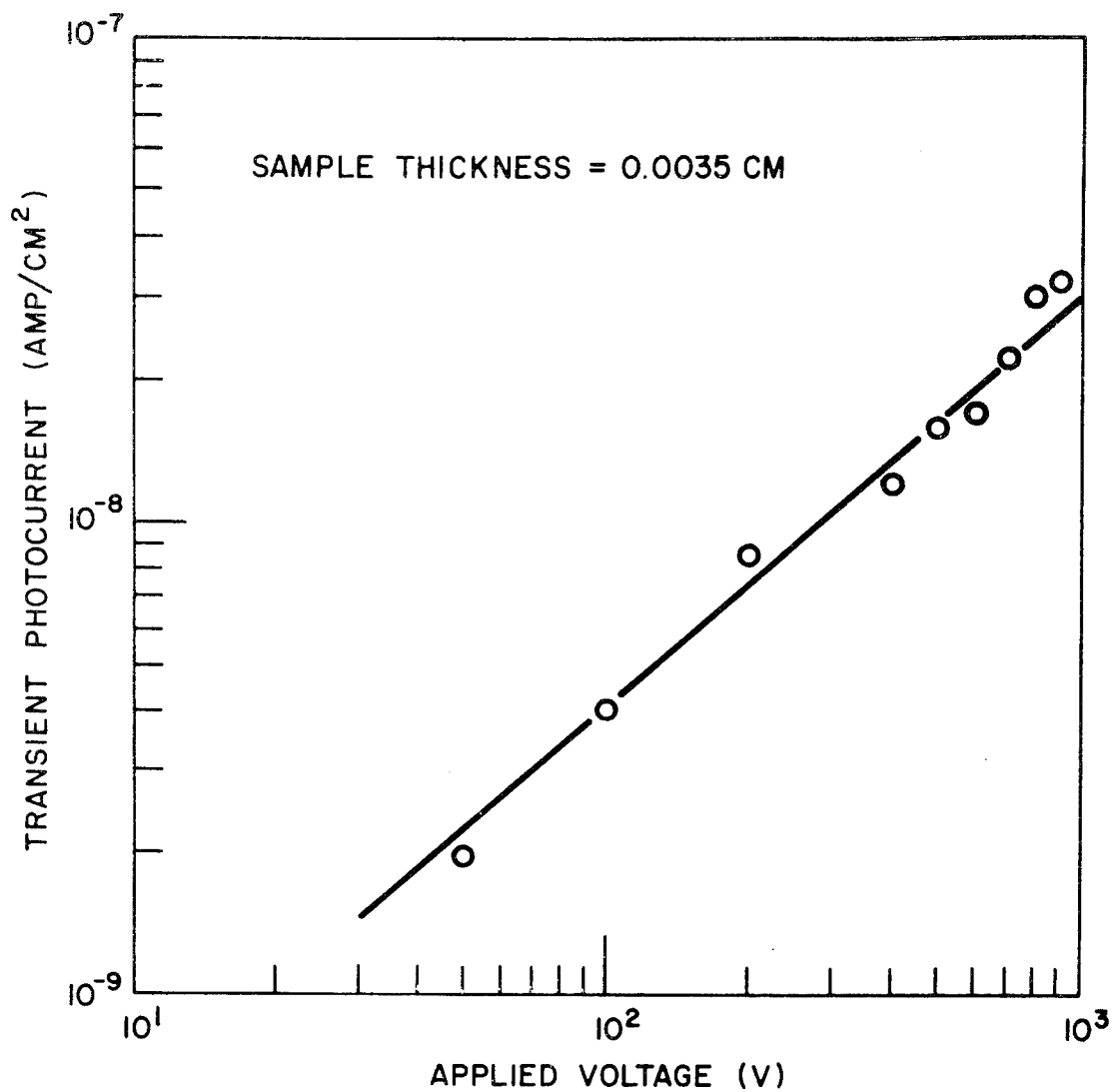


FIGURE 22 TRANSIENT PHOTOCURRENT-VOLTAGE CHARACTERISTICS (PMDA-DAB).

current-voltage characteristic was obtained for the PMDA-DAB sample. The current-voltage characteristics for the BTDA-DAB samples were superlinear indicating possibly the presence of space charge limited current effects.

If the mobility is on the order of  $1 \text{ cm}^2/\text{volt sec.}$ , the drift time would be too short to measure accurately with the thin samples used in these experiments. The studies were thus extended to a cast sample 0.127 mm thick and a sample 1 mm in thickness obtained by compacting several thin samples. A fast decaying signal was also obtained in these samples, however, and no drift time could be observed. The data on the transient photoconductivity studies are summarized in Table 3. In all cases investigated, the fast decay times of the transient photocurrent signal are indicative of severe charge carrier trapping.

### 3.4 RADIATION INDUCED CONDUCTIVITY MEASUREMENTS

The measurement procedure consisted of placing the sample at a known distance from the 4000 Curie Co-60 radiation source and applying a voltage to the sample to establish a steady dark current. Radiation was then allowed to fall on the sample causing the current to increase to a new level. After twenty to thirty seconds a steady state-radiation induced current was established. After recording this current value, the radiation was removed and the current level allowed to fall to its previous value. The current decayed about 90% of its value within 20-30 seconds. The procedure was then repeated for several applied voltages and also for zero volts applied. Data of this type were obtained at distances in the range 29 cm to 150 cm from the source. The radiation dose ranged from 33 rad/min to 900 rad/min.

The dark current level in the samples investigated was greater than radiation induced currents produced in the lead cables to the conductivity cell. Radiation induced currents produced with the samples present were thus interpreted as arising from the interaction of radiation with the Pyrrone polymer sample. Effects in the cell and lead assembly were investigated using teflon conductivity samples having a dark resistivity 2 orders of magnitude higher than the Pyrrone polymers investigated. Current-voltage characteristics illustrating radiation induced currents produced at the lowest and highest dose rates with both positive and negative voltage applied to the electrode receiving the incident radiation are shown for PMDA-DAB in Figure 23. A greater radiation current level was produced when a negative voltage was applied to the incident electrode. This was interpreted as being due to the motion of Compton electrons reinforcing the current due to the motion of free electrons in one direction (negative voltage) and subtracting from it in the other direction (positive voltage)(ref. 5). The free electrons are produced by interaction of the radiation with the material. Support for this interpretation was obtained from the observation that a net negative current was obtained in the sample with no applied field. This current arises from the motion of Compton electrons and is an effect associated with the momentum of impinging photons. Correcting the measured radiation induced current ( $I_R$ ) for this zero voltage current ( $I_0$ ) and the background dark current ( $I_D$ ) gave radiation induced currents,  $I_+ - I_0$  and  $I_- - I_0$ , that were

TABLE 3

TRANSIENT PHOTOCONDUCTION DATA ON PYRRONE SAMPLES

<u>BTDA-DAB</u>			
<u>Sample</u>	<u>Thickness (<math>\mu</math>)</u>	<u>Current-Voltage Relationship</u>	<u>Decay Time (<math>\mu</math> sec)</u>
7	20	Superlinear	28 $\rightarrow$ 35 (600 v $\rightarrow$ 50 v)
3	17.5	Superlinear	65.2 (600 v)
Several Samples Compacted	$\sim$ 1 mm	—	11.7 (700 v)
Cast Thick Sample	0.127 mm	—	13.4 (900 v)
<u>PMDA-DAB</u>			
<u>Sample</u>	<u>Thickness (<math>\mu</math>)</u>	<u>Current-Voltage Relationship</u>	<u>Decay Time (<math>\mu</math> sec)</u>
7	35.6	Linear	12-40 (900 v $\rightarrow$ 50 v)

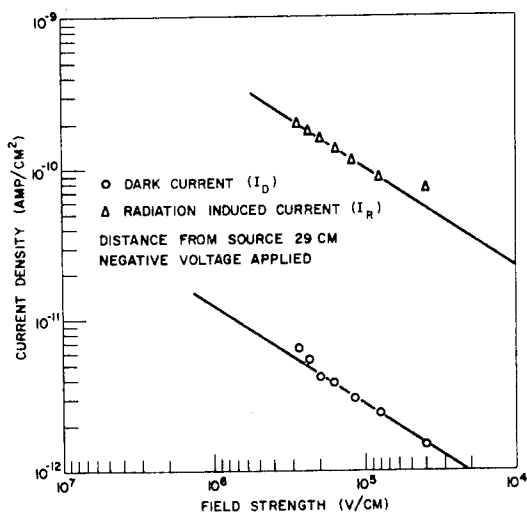
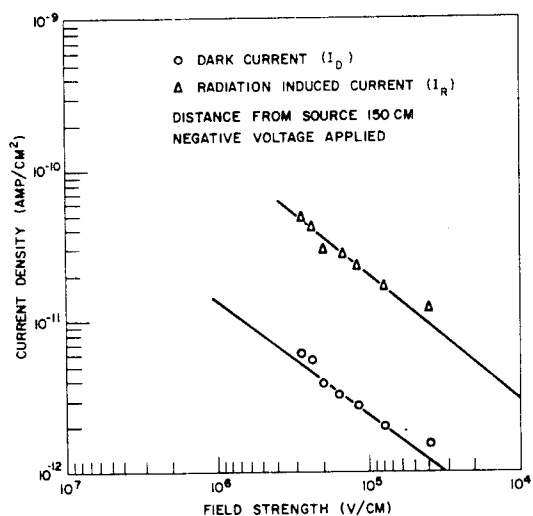
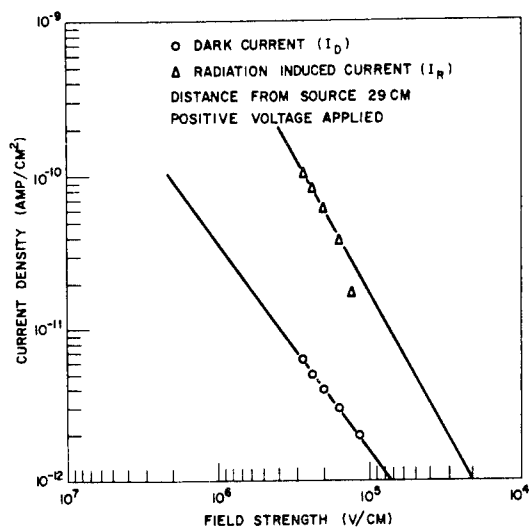
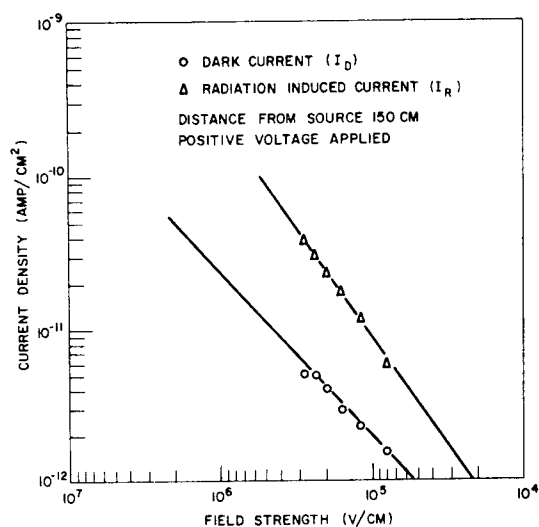


FIGURE 23 RADIATION INDUCED CURRENT CHARACTERISTICS (PMDA-DAB).

approximately symmetrical with respect to sign of applied voltage and increased sub-linearly with radiation dose rate. Tables 4 and 5 summarize radiation induced conductivity data for PMDA-DAB and BTDA-DAB respectively for an applied field strength of  $10^5$  volt/cm. For BTDA-DAB, radiation induced current i.e.  $I_+ - I_0$ ,  $I_- - I_0$ , was approximately 3 to 4 times smaller than that induced in PMDA-DAB.

The current due to the Compton effect was similar for both polymers. This resulted in net negative radiation-induced currents being measured when BTDA-DAB samples were irradiated with a positive voltage applied to the electrode receiving radiation. On correcting for  $I_0$ , however, it was found that the radiation induced current was again symmetrical with respect to sign of applied voltage as shown in Table 5.

Figure 24 shows the corrected radiation induced current plotted against radiation dose rate illustrating the sub-linear dependence. If  $I = K(D)^n$ , where  $I$  is the radiation induced current,  $D$  the dose rate and  $K$  a constant, the exponent  $n$  is 0.5.

### 3.5 EFFECT OF HIGH DOSES of 2 Mev ELECTRONS ON DARK CONDUCTIVITY AND PHOTO-CONDUCTIVITY

The procedure for evaluating the effect of high doses of 2 Mev electrons on the conductivity properties of PMDA-DAB and BTDA-DAB consisted of measuring current-voltage characteristics in the field strength range  $10^2$ - $10^6$  volt/cm and comparing the resultant data with similar data obtained on unirradiated samples. The conditions of measurement were chosen to approximate as closely as possible to those used in measuring unirradiated samples. The same light source was used for all measurements and was placed the same distance from the sample in all cases. Some variation in light intensity from sample to sample was caused by the variation in optical transmission of semitransparent electrodes. This transmission was measured in all cases allowing the actual intensity falling on the sample surface to be estimated. This value is recorded with the data for each sample. Figures 25 and 26 show conductivity data for PMDA-DAB and BTDA-DAB samples that were irradiated with  $1 \times 10^7$  rad at several temperatures. Figure 27 shows similar data for PMDA-DAB and BTDA-DAB samples that were irradiated with  $1 \times 10^9$  rad at  $20^\circ\text{C}$ . Current-voltage characteristics for PMDA-DAB and BTDA-DAB samples that were irradiated with  $5 \times 10^9$  rad at several temperatures are shown in Figures 28 and 29.

The radiated samples, in general, showed a higher dark current level when compared to unirradiated samples. Table 6 lists current levels obtained for irradiated samples at  $10^3$  volt/cm compared to unirradiated samples. The observed increase in the case of BTDA-DAB was much less than that in PMDA-DAB, the dark current for irradiated samples in no case being more than a factor of five above that of the unirradiated samples. The dark current level was much greater in the case of irradiated PMDA-DAB, being a factor of 10 to 1000 above that of the unirradiated samples. The effect of temperature at which the radiation was accumulated was such that the dark current increase was highest at the lowest temperature for PMDA-DAB with a constant radiation dose. In the case of BTDA-DAB no significant influence of temperature was found on the dark current



TABLE 4

## RADIATION INDUCED CURRENT DATA FOR PMDA-DAB

FIELD STRENGTH =  $10^5$  V/CM  
CURRENTS IN AMP/CM<sup>2</sup> X  $10^{11}$

Distance from Source (cm)	Dose Rate (rad/min)	POSITIVE VOLTAGE APPLIED				NEGATIVE VOLTAGE APPLIED				ZERO VOLTAGE APPLIED	
		$I_R$	$I_D$	$I_+$	$I_+ - I_0$	$I_R$	$I_D$	$I_-$	$I_- - I_0$	$I_0$	$I_0$
150	33	+ 0.88	+ 0.20	+ 0.68	+ 1.28	- 2.0	- 0.24	- 1.76	- 1.16	- 0.60	- 0.60
150	33	+ 3.40	+ 2.80	+ 0.60	+ 1.44	- 4.75	- 2.60	- 2.15	- 1.31	- 0.84	- 0.84
100	80	+ 1.56	+ 0.28	+ 1.28	+ 1.88	- 2.45	- 0.38	- 2.07	- 1.47	- 0.60	- 0.60
75	120	+ 1.80	+ 0.22	+ 1.58	+ 2.25	- 2.90	- 0.26	- 2.64	- 1.97	- 0.67	- 0.67
50	350	+ 1.60	+ 0.21	+ 1.39	+ 2.34	- 5.40	- 0.27	- 5.13	- 4.18	- 0.95	- 0.95
29	900	+ 1.65	+ 0.15	+ 1.50	+ 3.95	- 10.00	- 0.27	- 9.73	- 6.28	- 2.45	- 2.45

$I_R$  = Measured current in Radiant Field with voltage applied.

$I_D$  = Dark current before and after irradiation with voltage applied.

$$I_+, I_- = I_R - I_D$$

$I_0$  = Current measured in Radiant Field with no voltage applied.

Radiation was incident upon the electrode to which the voltage was applied; a sandwich arrangement was used for all measurements.

TABLE 5

## RADIATION INDUCED CURRENT DATA FOR BTDA-DAB

Distance from Source (cm)	Dose Rate (rad/min)	FIELD STRENGTH = $10^5$ V/CM		CURRENTS IN AMP/CM <sup>2</sup> $\times 10^{12}$				ZERO VOLTAGE APPLIED
		POSITIVE VOLTAGE APPLIED		NEGATIVE VOLTAGE APPLIED				
		$I_R - I_o$	$I_D$	$I_+ - I_o$	$I_R - I_o$	$I_D$	$I_- - I_o$	
150	33	+ 4.3	+ 0.97	+ 3.33	- 3.1	- 1.13	- 1.97	- 7.4
100	80	+ 5.2	+ 0.73	+ 4.47	- 6.1	- 1.18	- 4.92	- 6.0
75	120	+ 7.7	+ 0.87	+ 6.83	- 6.9	- 1.0	- 5.9	- 8.3
75	120	+ 6.8	+ 0.7	+ 6.1	- 8.0	- 0.78	- 7.22	- 8.3
50	350	+ 8.0	+ 0.58	+ 7.42	- 13.0	- 1.0	- 12.0	- 15
29	900	+ 15.7	+ 0.35	+ 15.35	- 21.9	- 1.44	- 20.46	- 42

$I_R$  = Measured current in Radiant Field and Voltage applied.

$I_D$  = Dark current before and after irradiation with voltage applied.

$I_+$ ,  $I_-$  =  $I_R - I_D$

$I_O$  = Current measured in Radiant Field with no voltage applied.

Radiation was incident upon the electrode to which the voltage was applied; a sandwich arrangement was used for all measurements.

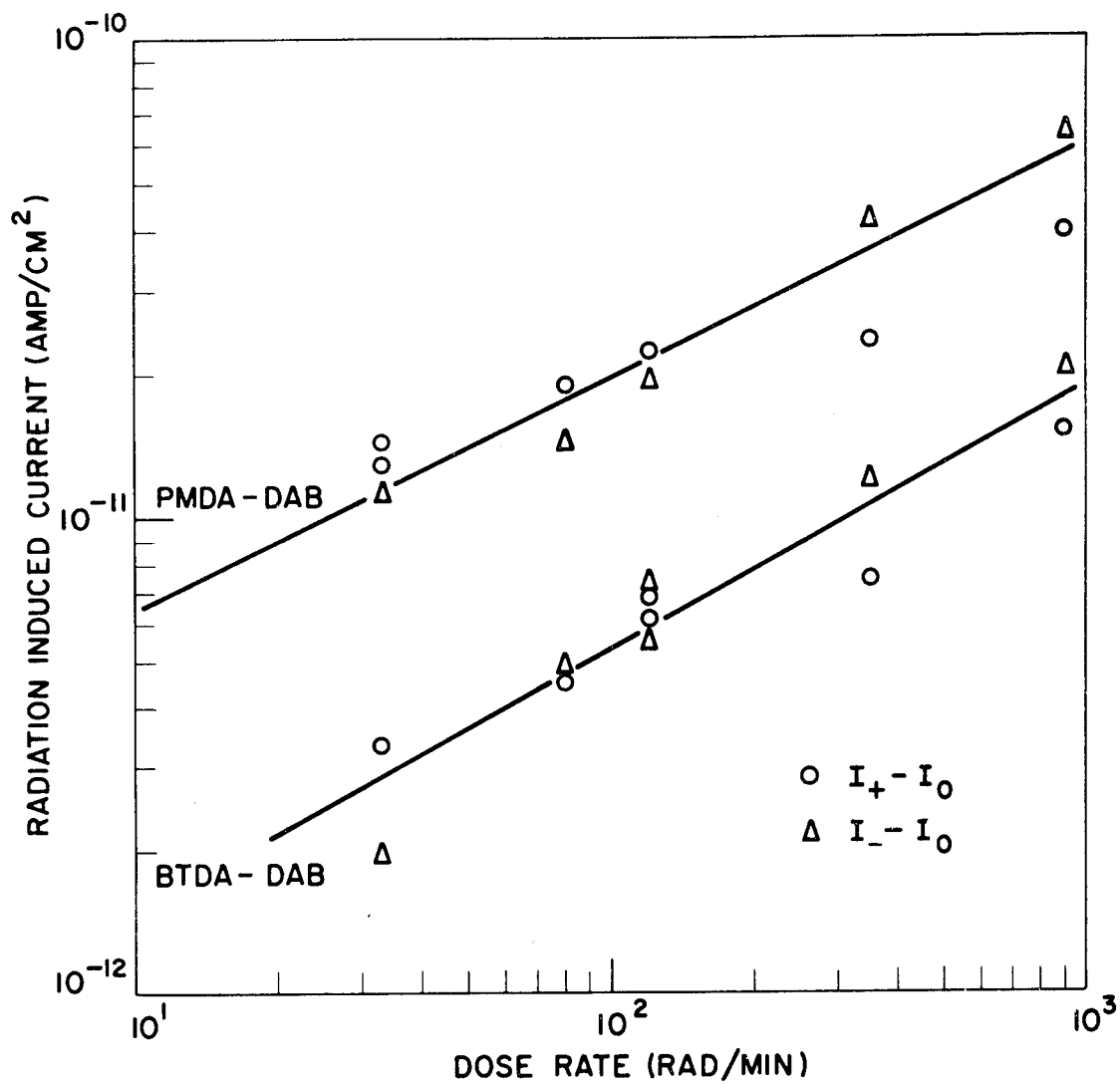


FIGURE 24 RADIATION INDUCED CURRENT AS A FUNCTION OF RADIATION DOSE RATE FOR PMDA-DAB AND BTDA-DAB.

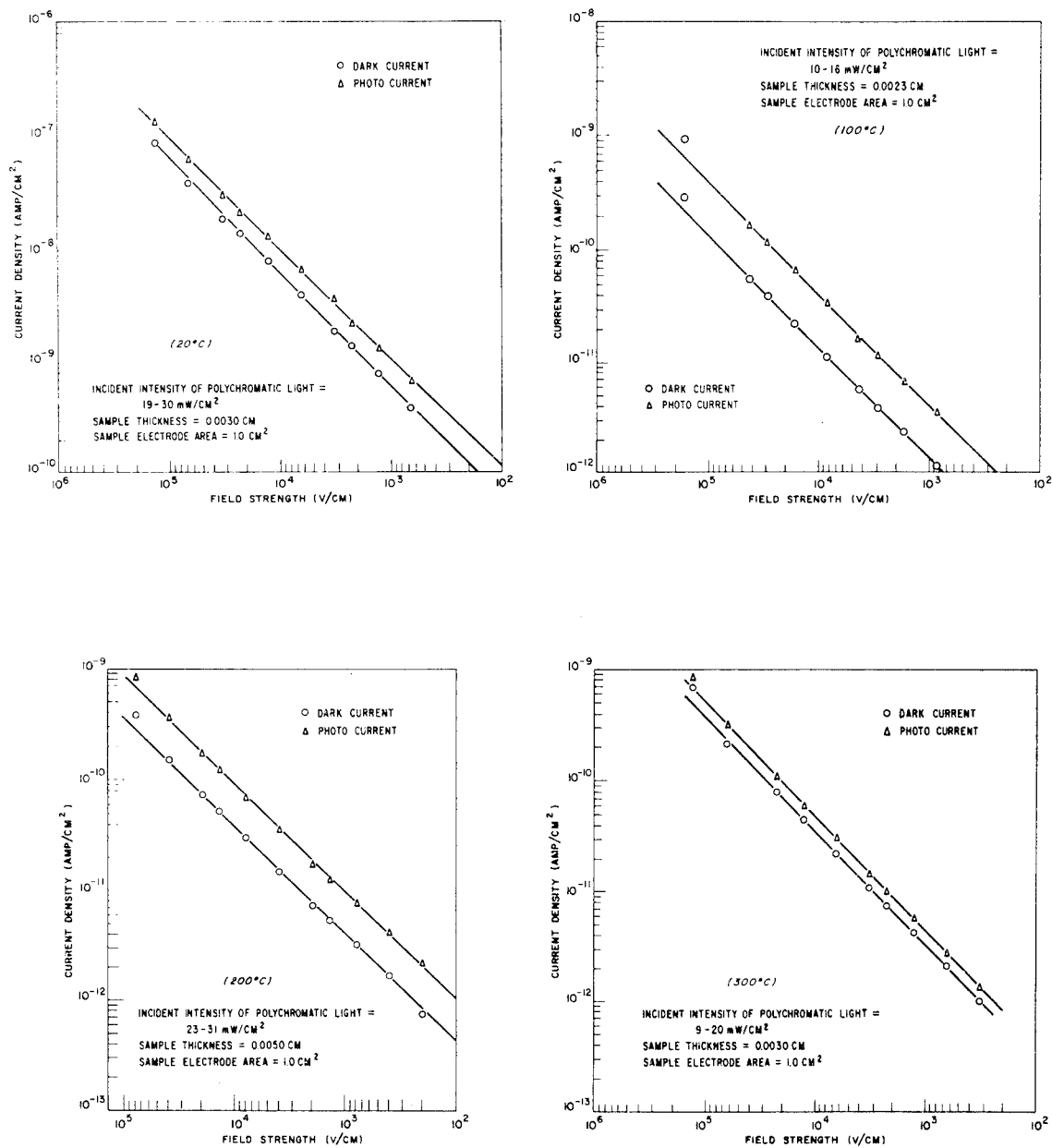


FIGURE 25 CURRENT-VOLTAGE CHARACTERISTICS OF IRRADIATED PMDA-DAB SAMPLES (RADIATION DOSE =  $1 \times 10^7$  RAD AT VARIOUS TEMPERATURES).

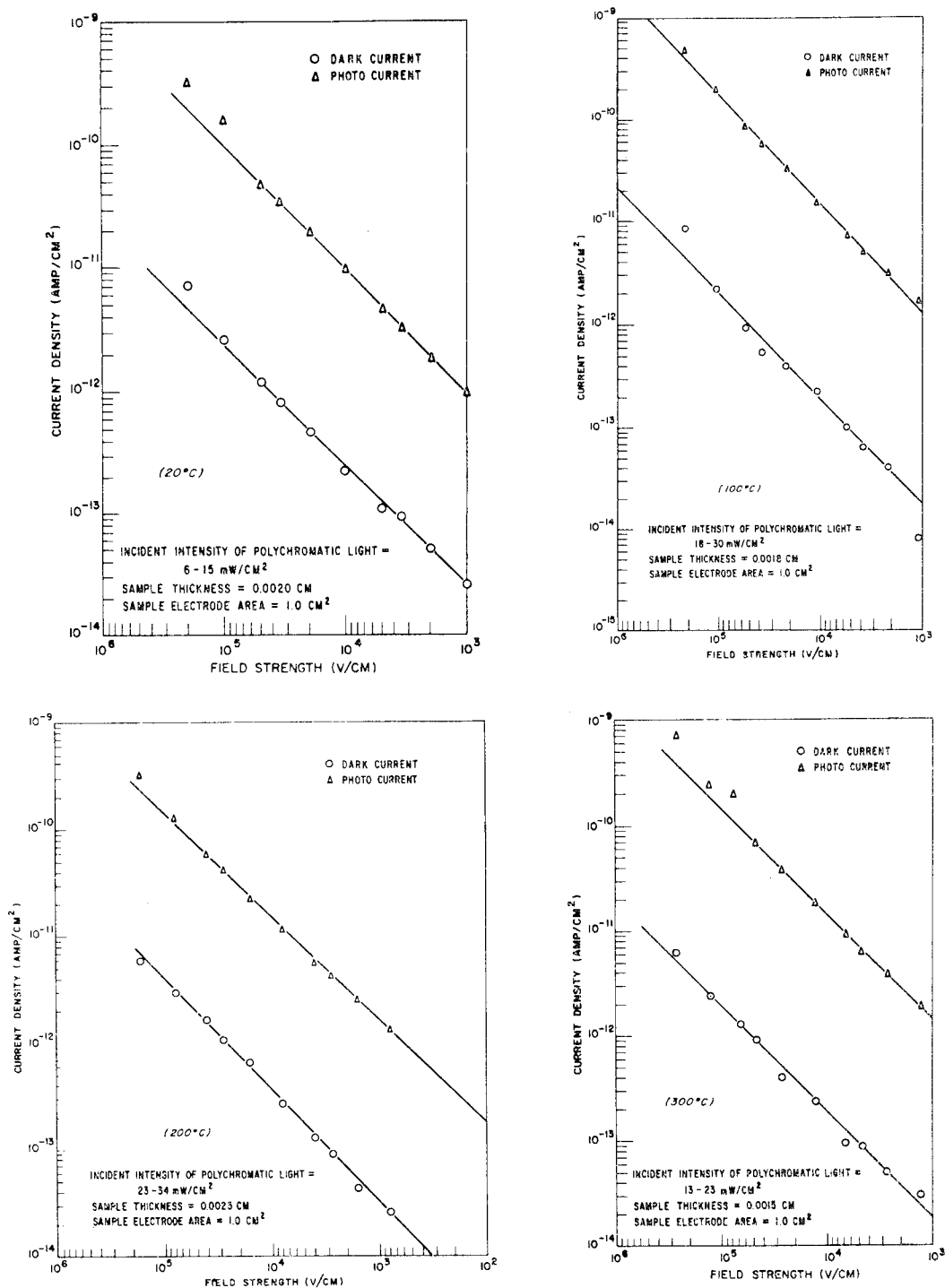


FIGURE 26 CURRENT-VOLTAGE CHARACTERISTICS OF IRRADIATED BTDA-DAB SAMPLES (RADIATION DOSE =  $1 \times 10^7$  RAD AT VARIOUS TEMPERATURES).

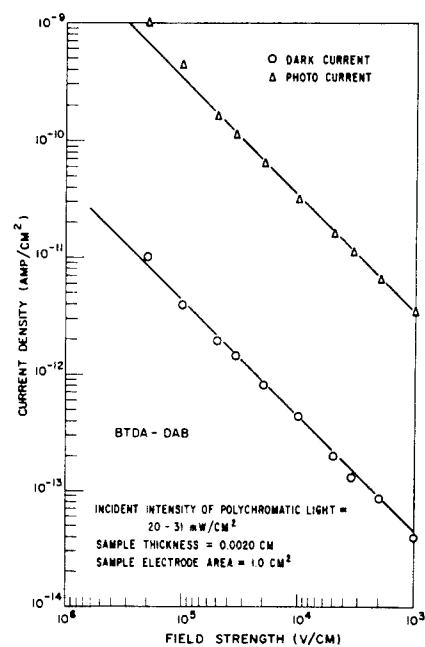
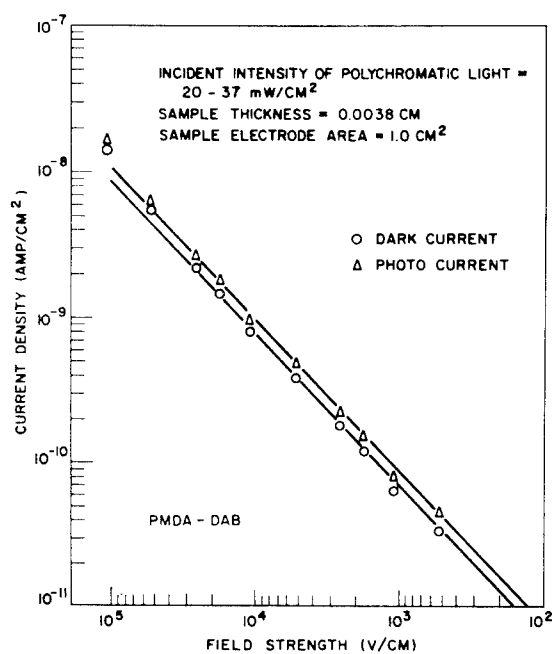


FIGURE 27 CURRENT-VOLTAGE CHARACTERISTICS OF IRRADIATED PMDA-DAB AND BTDA-DAB SAMPLES (RADIATION DOSE =  $1 \times 10^9$  RAD AT 20°C).

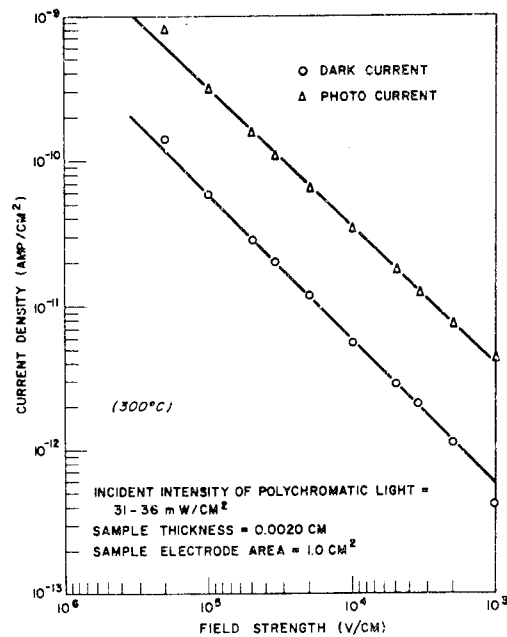
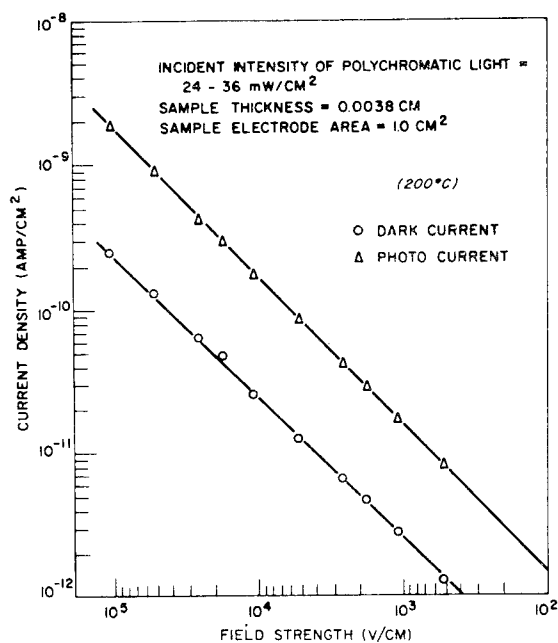
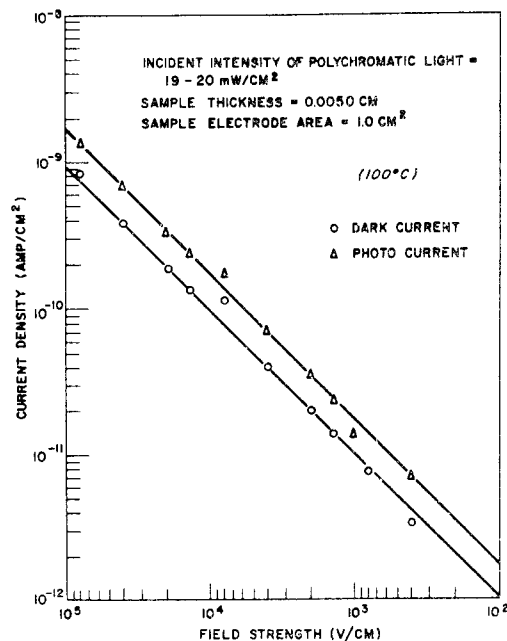
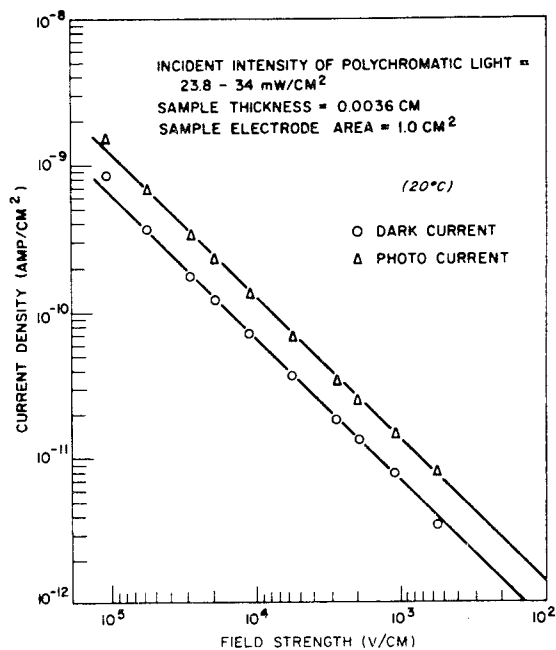


FIGURE 28 CURRENT-VOLTAGE CHARACTERISTICS OF IRRADIATED PMDA-DAB SAMPLES (RADIATION DOSE =  $5 \times 10^9$  RAD AT VARIOUS TEMPERATURES).

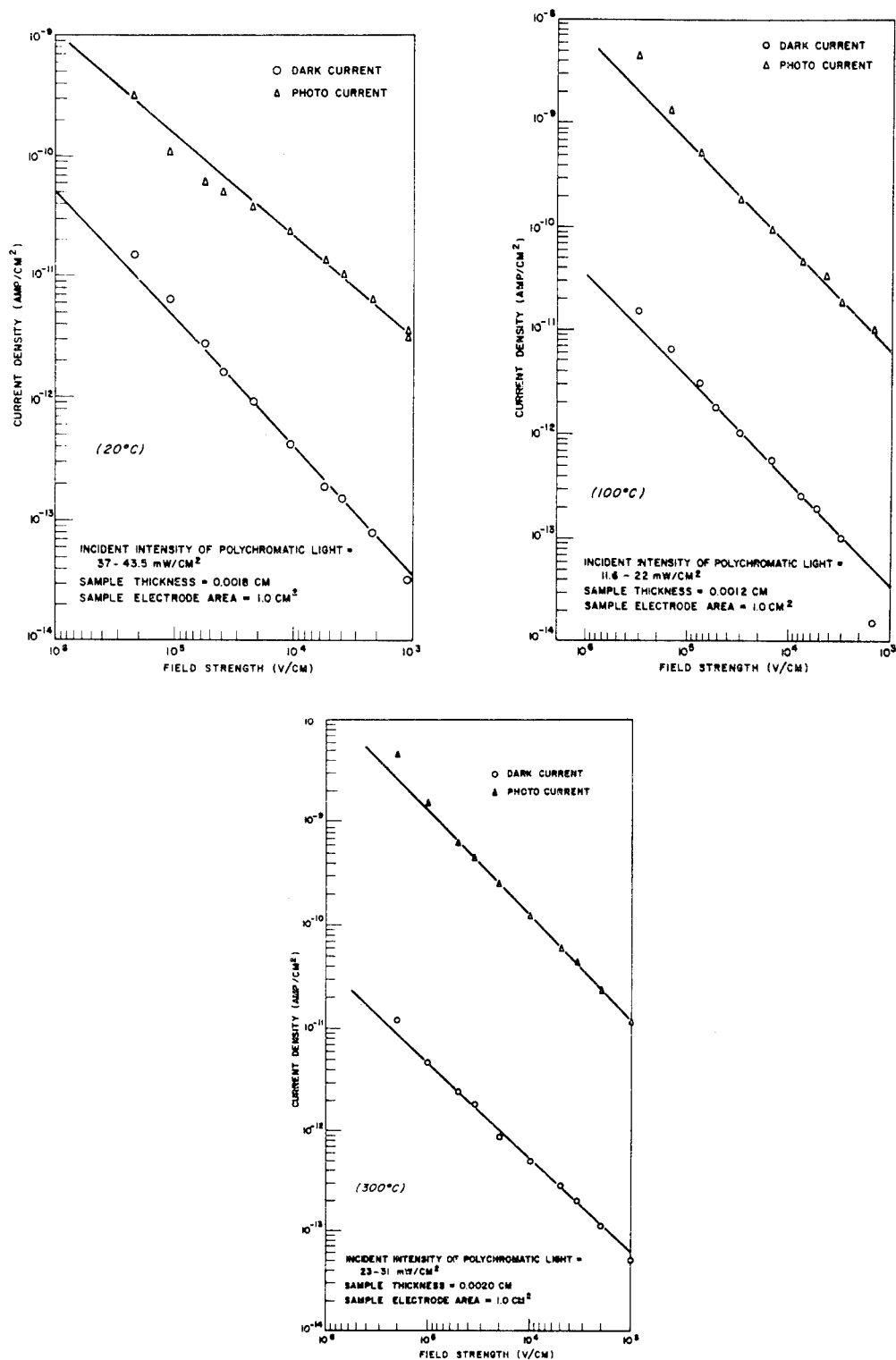


FIGURE 29 CURRENT-VOLTAGE CHARACTERISTICS OF IRRADIATED BTDA-DAB SAMPLES (RADIATION DOSE =  $5 \times 10^9$  RAD AT VARIOUS TEMPERATURES).



TABLE 6

DARK AND PHOTOCURRENT LEVEL AT  $10^3$  VOLT/CM FOR IRRADIATED PYRONE SAMPLES

		PMDA-DAB				BTDA-DAB			
		Photocurrent ( $I_p$ ) ( $I_p$ ) amp/cm <sup>2</sup>	Dark Current ( $I_D$ ) ( $I_D$ ) amp/cm <sup>2</sup>	$I_p - I_D$ amp/cm <sup>2</sup>	Photocurrent ( $I_p$ ) amp/cm <sup>2</sup>	Dark Current ( $I_D$ ) amp/cm <sup>2</sup>	$I_p - I_D$ amp/cm <sup>2</sup>		
Unirradiated		$2.5 \times 10^{-12}$	$8 \times 10^{-14}$	$2.42 \times 10^{-12}$	$2 \times 10^{-12}$	$9 \times 10^{-15}$	$2 \times 10^{-12}$		
$1 \times 10^7$ rad	20°	$1 \times 10^{-9}$	$6 \times 10^{-10}$	$4 \times 10^{-10}$	$1 \times 10^{-12}$	$2.5 \times 10^{-14}$	$1 \times 10^{-12}$		
	100°C	$4 \times 10^{-12}$	$1.4 \times 10^{-12}$	$2.6 \times 10^{-12}$	$1.1 \times 10^{-12}$	$1.7 \times 10^{-14}$	$1.1 \times 10^{-12}$		
	200°C	$9.8 \times 10^{-12}$	$4 \times 10^{-12}$	$5.8 \times 10^{-12}$	$1.7 \times 10^{-12}$	$3.2 \times 10^{-14}$	$1.7 \times 10^{-12}$		
	300°C	$4.2 \times 10^{-12}$	$3 \times 10^{-12}$	$1.2 \times 10^{-12}$	$1.5 \times 10^{-12}$	$2 \times 10^{-14}$	$1.5 \times 10^{-12}$		
$1 \times 10^9$ rad	20°C	$8 \times 10^{-11}$	$7 \times 10^{-11}$	$1 \times 10^{-11}$	$3.5 \times 10^{-12}$	$4 \times 10^{-14}$	$3.5 \times 10^{-12}$		
$5 \times 10^9$ rad	20°C	$1.4 \times 10^{-11}$	$7 \times 10^{-12}$	$7 \times 10^{-12}$	$3.5 \times 10^{-12}$	$3 \times 10^{-14}$	$3.5 \times 10^{-12}$		
	100°C	$1.6 \times 10^{-11}$	$1 \times 10^{-11}$	$6 \times 10^{-12}$	$6 \times 10^{-12}$	$3 \times 10^{-14}$	$6 \times 10^{-12}$		
	200°C	$1.5 \times 10^{-11}$	$3 \times 10^{-12}$	$1.2 \times 10^{-11}$	—	—	—		
	300°C	$3.5 \times 10^{-12}$	$6 \times 10^{-13}$	$2.9 \times 10^{-12}$	$1.2 \times 10^{-11}$	$5 \times 10^{-14}$	$1.2 \times 10^{-11}$		

increase produced. All samples showed photoconductivity on illumination, the net increase in current produced i.e.  $I_p - I_d$ , falling in the range  $10^{-12}$ – $10^{-11}$  amps for all samples but one PMDA-DAB sample. This sample had accumulated  $10^7$  rad at 20°C and had abnormally high photocurrent and dark current. In the case of BTDA-DAB the photocurrent-dark current ratio was little changed from that observed for unirradiated samples. The photocurrent-dark current ratio for PMDA-DAB was generally much reduced compared to unirradiated samples in view of the increased dark current level.

In summary, the effect of high radiation doses of 2 Mev electrons on the conductivity properties of Pyrrone polymers was found to be more marked in the case of PMDA-DAB, the main effect being an increased dark current level and reduced photocurrent-dark current ratio. In the case of BTDA-DAB the effect of radiation was minor. The main effect observed was a slight increase in dark current level.

### 3.6 DIELECTRIC CONSTANT AND LOSS AS A FUNCTION OF FREQUENCY AND TEMPERATURE

Measurement of dielectric constant and dissipation factor for PMDA-DAB and BTDA-DAB as a function of temperature and frequency was carried out after first cycling the sample to 300°C in vacuo. This procedure was found necessary in order to avoid erratic results. After the first cycle in vacuum the dielectric constant and dissipation factor curves were found to be reproducible. Dielectric constant as a function of temperature at four frequencies is shown in Figures 30 and 31 for PMDA-DAB and BTDA-DAB. Percent dissipation factor as a function of temperature at four frequencies is shown in Figures 32 and 33 for PMDA-DAB and BTDA-DAB.

At all frequencies very little change was found in dielectric constant at temperatures up to 150–200°C. At this temperature there was a tendency for dielectric constant to increase rapidly with increasing temperature at the low frequency. At the higher frequency the dielectric constant decreased with increasing temperature. This type of behavior has been reported for Kapton (ref. 6). At 1% expansion of the film at 200°C could explain the observed behavior in BTDA-DAB, requiring a coefficient of linear expansion of  $5 \times 10^{-5} \text{ deg}^{-1}$ . The value reported for the linear expansion coefficient of Kapton below room temperature is about half this (ref. 6). Either the thermal expansion is greater in the Pyrrone polymers, or there is a second order transition above room temperature but below 200°C. Thermal shrinkage and expansion data are necessary for further explanation of this behavior.

Dissipation factor was also little changed by temperature until temperatures higher than 150°C were attained. Above this temperature large increases were obtained. The dependence of dissipation factor upon frequency indicates a large activation energy for the relaxation process. The activation energy was estimated to be  $> 1.1 \text{ eV}$  for both Pyrrones by plotting the frequency at which the dissipation factor becomes 3% versus  $\frac{1}{T^\circ K}$ . This result is consistent with the direct-current conductivity data.

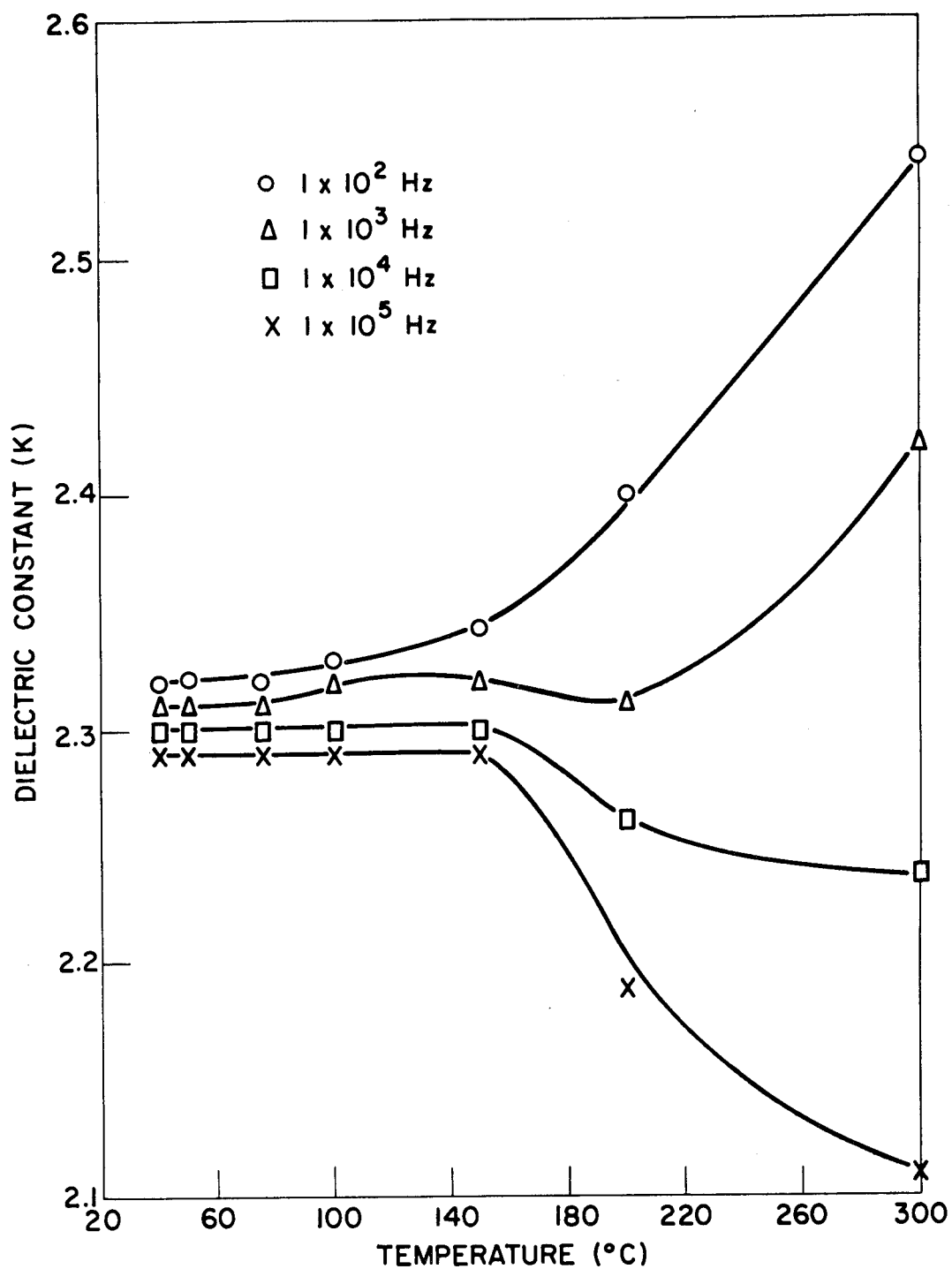


FIGURE 30 DIELECTRIC CONSTANT OF PMDA-DAB.

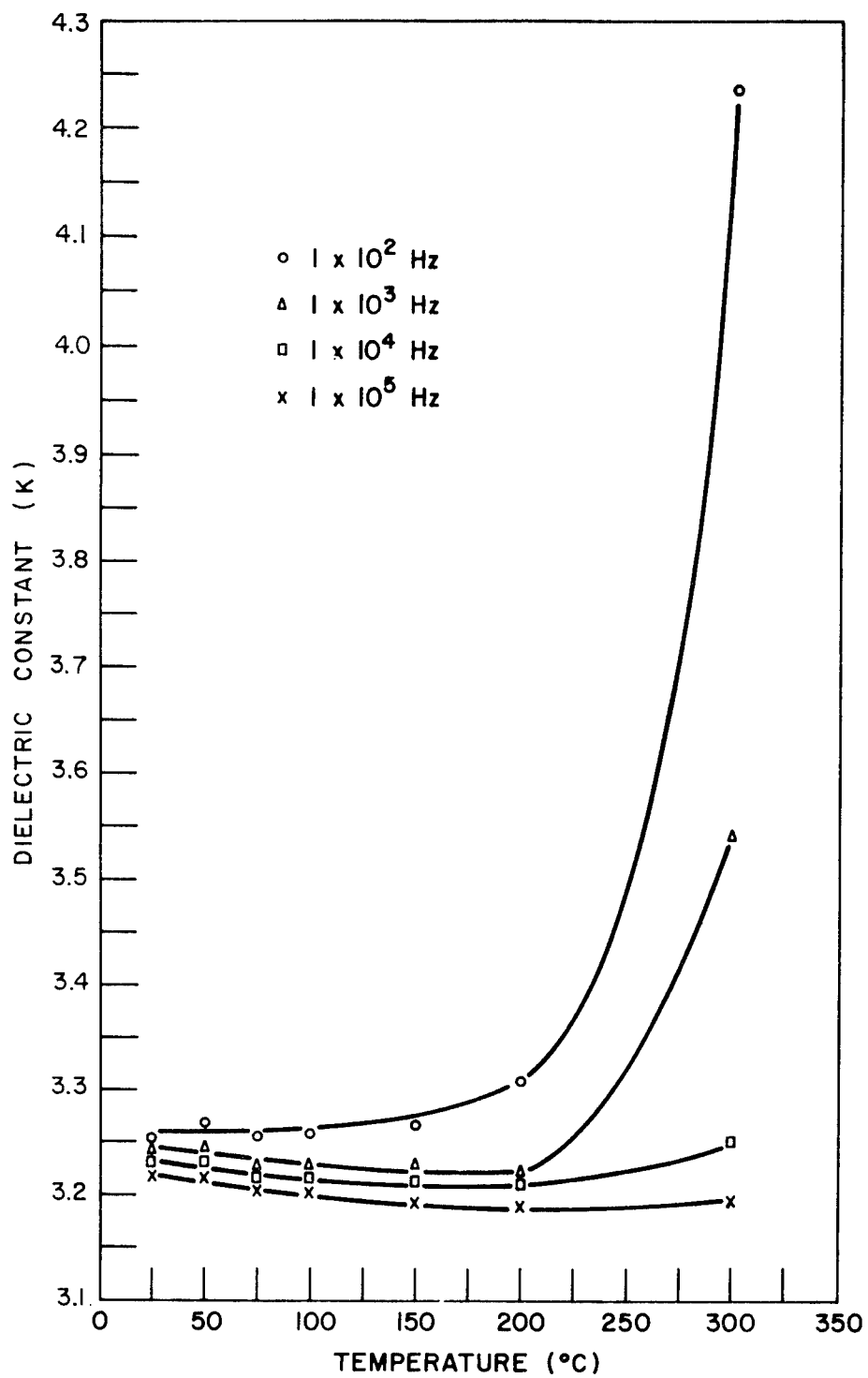


FIGURE 31 DIELECTRIC CONSTANT OF BTDA-DAB.

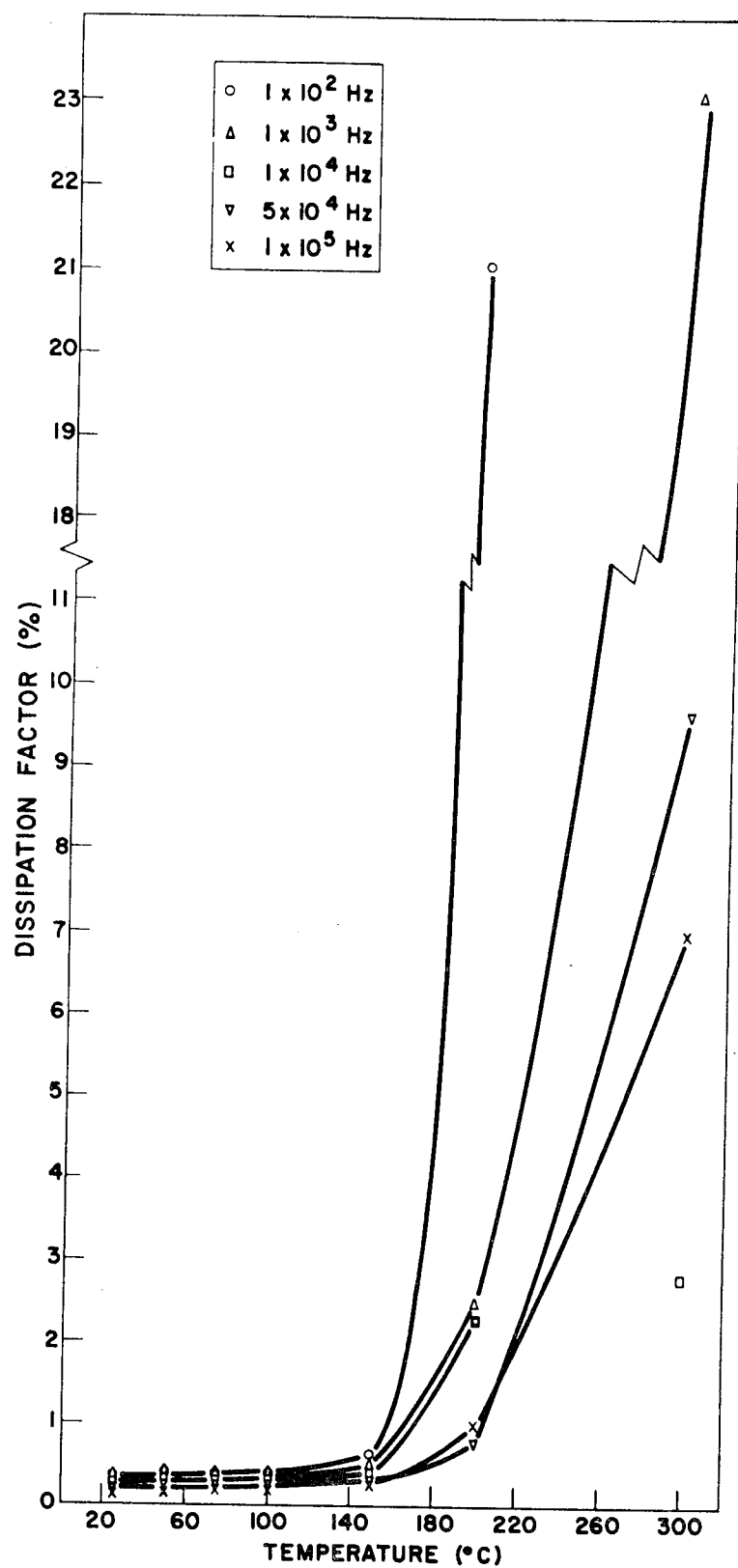


FIGURE 32 DIELECTRIC LOSS OF PMDA-DAB.

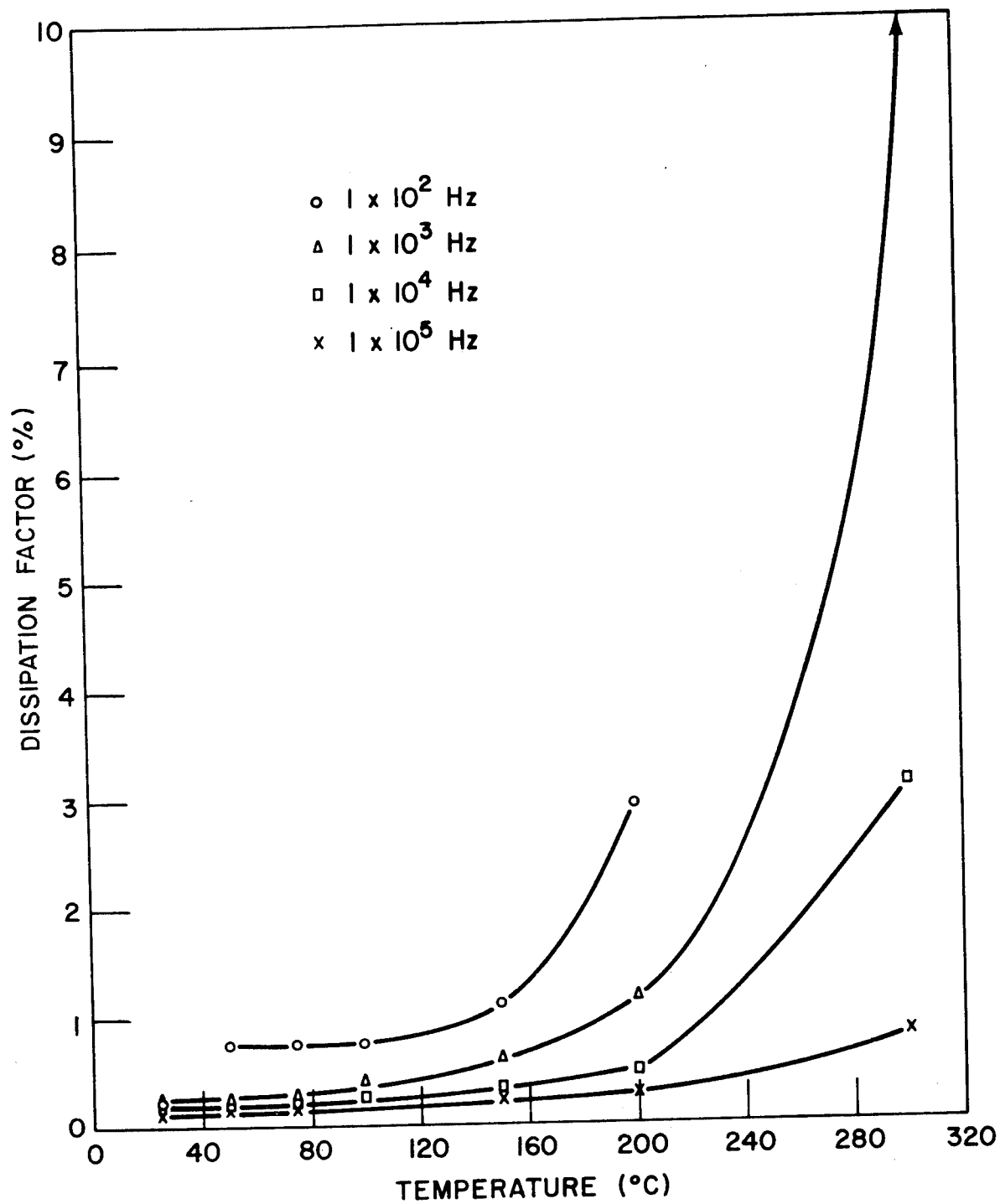


FIGURE 33 DIELECTRIC LOSS OF BTDA-DAB.

### 3.7 EFFECT OF HIGH DOSES OF 2 Mev ELECTRONS ON DIELECTRIC PROPERTIES

Dielectric constant and dissipation factor data for irradiated samples of PMDA-DAB and BTDA-DAB are given in Tables 7 and 8 respectively. The measurements were carried out at room temperature. In general no marked effect of radiation could be seen on comparing the results with similar data obtained on unirradiated samples under the same conditions (also shown in Tables 7 and 8). The unirradiated polymer samples used as controls had dissipation factors similar to those found in irradiated samples. The fairly high losses found in these samples are not necessarily typical; those in Figures 31 and 32 were much lower. The dielectric constant variations fall within the range of values obtained for several samples of these polymer films. The variations are due to errors in measuring sample thickness. In summary, high accumulated doses of 2 Mev electrons appear to have negligible effect on the dielectric constant and dissipation factor of both Pyrrone polymers investigated.

### 4. GENERAL CONCLUSIONS

Pyrrone polymers BTDA-DAB, cast in films from solution and cured for at least 24 hours at 300°C exhibited the following electrical characteristics:

1. The dark resistivity was on the order of  $10^{15}$ - $10^{17}$  ohm-cm. PMDA-DAB samples tended to fall on the low end of this range. BTDA-DAB samples generally fell in the high extremity of this range.
2. With evaporated gold electrodes, dark current was linear with applied voltage i.e. obeyed Ohm's law, up to field strengths approaching  $10^6$  volt/cm.
3. Both polymers displayed photoconductivity, photocurrent-dark current ratios of 200-300 being obtained for BTDA-DAB and 40-60 for PMDA-DAB with polychromatic uv-visible light having intensity 20-30 mw/cm<sup>2</sup>.
4. The temperature dependence of both dark and photocurrent in the temperature range 20-300°C i.e. non-linear  $\log(\text{current}) - \frac{1}{T^\circ K}$  plots, implied that more than one mechanism for charge carrier generation was operating in this temperature range.
5. The photocurrent spectral dependence was related to the absorption spectrum of the two polymers. Peak photoconductivity at constant illumination intensity was found in the visible region at 610 mμ for PMDA-DAB and 500 mμ for BTDA-DAB. Measurable photocurrents could be detected at wavelengths extending into the infrared ( $> 1 \mu$ ).
6. Transient photocurrent studies showed evidence for severe charge-carrier trapping.

TABLE 7

## DIELECTRIC PROPERTIES OF IRRADIATED PMDA-DAB

No Irradiation				$5 \times 10^9$ rad at 300°C			
Frequency (Hz)	Dissipation Factor	Capacitance (pf)	<u>K</u>	Frequency (Hz)	Dissipation Factor	Capacitance (pf)	<u>K</u>
100	$5 \times 10^{-2}$	105	4.5	100	$2 \times 10^{-2}$	230	3.6
1 K	$4 \times 10^{-2}$	99	4.2	1 K	$2 \times 10^{-2}$	223	3.5
10 K	$4 \times 10^{-2}$	93	4.0	10 K	$1.7 \times 10^{-2}$	217	3.4
100 K	$3 \times 10^{-2}$	90	3.9	100 K	$1.6 \times 10^{-2}$	210	3.3
$5 \times 10^9$ rad at 200°C				$5 \times 10^9$ rad at 100°C			
Frequency (Hz)	Dissipation Factor	Capacitance (pf)	<u>K</u>	Frequency (Hz)	Dissipation Factor	Capacitance (pf)	<u>K</u>
100	$4 \times 10^{-2}$	180	5.2	100	$5 \times 10^{-2}$	110	6.3
1 K	$4 \times 10^{-2}$	168	4.8	1 K	$4 \times 10^{-2}$	100	5.7
10 K	$3.1 \times 10^{-2}$	159	4.6	10 K	$3.3 \times 10^{-2}$	95.2	5.4
100 K	$1 \times 10^{-2}$	151	4.3	100 K	$3 \times 10^{-2}$	90	5.2
$5 \times 10^9$ rad at 20°C				$1 \times 10^9$ rad at 20°C			
Frequency (Hz)	Dissipation Factor	Capacitance (pf)	<u>K</u>	Frequency (Hz)	Dissipation Factor	Capacitance (pf)	<u>K</u>
100	$5 \times 10^{-2}$	144	5.0	100	$5 \times 10^{-2}$	140	5.2
1 K	$4 \times 10^{-2}$	133	4.6	1 K	$5 \times 10^{-2}$	131	4.9
10 K	$3 \times 10^{-2}$	127	4.4	10 K	$4 \times 10^{-2}$	120	4.5
100 K	$2.5 \times 10^{-2}$	122	4.2	100 K	$3 \times 10^{-2}$	113	4.2
$1 \times 10^8$ rad at 20°C							
Frequency (Hz)	Dissipation Factor	Capacitance (pf)	<u>K</u>				
100	$3 \times 10^{-2}$	99	4.0				
1 K	$2 \times 10^{-2}$	96	3.9				
10 K	$2 \times 10^{-2}$	93	3.8				
100 K	$2 \times 10^{-2}$	90	3.7				



TABLE 8

## DIELECTRIC PROPERTIES OF IRRADIATED BTDA-DAB

No Irradiation				5 x 10 <sup>9</sup> rad at 300°C			
Frequency (Hz)	Dissipation Factor	Capacitance (pf)	<u>K</u>	Frequency (Hz)	Dissipation Factor	Capacitance (pf)	<u>K</u>
100	1 x 10 <sup>-2</sup>	148	3.1	100	1 x 10 <sup>-2</sup>	192	3.3
1 K	1 x 10 <sup>-2</sup>	176	3.0	1 K	1 x 10 <sup>-2</sup>	189	3.3
10 K	1 x 10 <sup>-2</sup>	173	3.0	10 K	1 x 10 <sup>-2</sup>	186	3.2
100 K	1 x 10 <sup>-2</sup>	168	2.9	100 K	8 x 10 <sup>-3</sup>	184	3.2
5 x 10 <sup>9</sup> rad at 100°C				5 x 10 <sup>9</sup> rad at 20°C			
Frequency (Hz)	Dissipation Factor	Capacitance (pf)	<u>K</u>	Frequency (Hz)	Dissipation Factor	Capacitance (pf)	<u>K</u>
100	9 x 10 <sup>-3</sup>	253	3.6	100	7 x 10 <sup>-3</sup>	205	3.5
1 K	9 x 10 <sup>-3</sup>	250	3.6	1 K	7 x 10 <sup>-3</sup>	203	3.5
10 K	1.4 x 10 <sup>-2</sup>	246	3.5	10 K	7 x 10 <sup>-3</sup>	201	3.4
100 K	1 x 10 <sup>-2</sup>	239	3.4	100 K	7 x 10 <sup>-3</sup>	199	3.4
1 x 10 <sup>9</sup> rad at 20°C				1 x 10 <sup>8</sup> rad at 20°C			
Frequency (Hz)	Dissipation Factor	Capacitance (pf)	<u>K</u>	Frequency (Hz)	Dissipation Factor	Capacitance (pf)	<u>K</u>
100	1 x 10 <sup>-2</sup>	158	3.2	100	2 x 10 <sup>-2</sup>	203	2.9
1 K	1 x 10 <sup>-2</sup>	155	3.1	1 K	2 x 10 <sup>-2</sup>	198	2.8
10 K	1 x 10 <sup>-2</sup>	153	3.1	10 K	2 x 10 <sup>-2</sup>	192	2.8
100 K	1 x 10 <sup>-2</sup>	151	3.0	100 K	2 x 10 <sup>-2</sup>	186	2.7

7. When gamma radiation at dose rates in the range 10-1000 rad/min was allowed to fall on polymer samples, the radiation produced currents ranging from  $1 \times 10^{-11}$  to  $6 \times 10^{-11}$  amp/cm<sup>2</sup> in PMDA-DAB and from  $2 \times 10^{-12}$  to  $2 \times 10^{-11}$  amp/cm<sup>2</sup> in BTDA-DAB at  $10^5$  volt/cm. In addition to these currents, which arise from the motion of free radiation induced charge carriers migrating in the electric field, a current component arising from the motion of Compton electrons ranging from  $6 \times 10^{-12}$  to  $4 \times 10^{-11}$  amp/cm<sup>2</sup> was produced. This current component reinforced the radiation induced current obtained when a negative voltage was applied to the electrode upon which radiation was incident and subtracted from the positive current. A sub-linear dependence of radiation induced current on dose rate was found.

8. Both dielectric constant and dissipation factor showed little change with temperature up to 150°C at frequencies ranging from  $10^2$ - $10^5$  Hz. Above this temperature the dielectric constant increased with increasing temperature at the lower frequency and decreased with increasing temperature at the higher frequency. Large increases in dissipation factor at temperatures exceeding 150°C also occurred. The activation energy for the relaxation process at these temperatures was found to be similar to the activation energy for dark conduction.

9. The effect of accumulated doses of 2 Mev electrons ranging from  $1 \times 10^7$  rad to  $5 \times 10^9$  rad in the temperature range 20°C to 300°C was generally to cause an increased dark current level. This resulted in a decreased photocurrent-dark current ratio. The dark current level increase in BTDA-DAB was found to be no more than a factor of 5. In the case of PMDA-DAB, dark current level increases ranged from a factor of 10 to 1000. At a constant radiation dose it was found that the effect of radiation was more marked at the lowest temperatures at which radiation was accumulated. Thus, samples that accumulated radiation-dose at 300°C showed electrical characteristics similar to those of unirradiated specimens.

High doses of 2 Mev electrons were found to have a minor effect on the dielectric constant and dissipation factor, measured at room temperature. A slight increase in dissipation factor was observed that may not have been significant since it fell within the range of dissipation factor values obtained for unirradiated samples.

#### REFERENCES

1. (a) G. F. Pezdirtz and V. L. Bell, NASA TND3148, December 1965;  
(b) V. L. Bell and G. F. Pezdirtz, Polymer Letters 3, 977 (1965).
2. V. L. Bell and R. A. Jewell, J. Polymer Sci., A1, 5, 3043 (1967).
3. P. J. Reucroft, O. N. Rudyj and M. M. Labes, Molecular Crystals 1, 429 (1966).
4. R. G. Kepler, Phys. Rev. 119, 1226 (1960).
5. R. A. Meyer, F. L. Bouquet and R. S. Alger, J. Appl. Phys. 27, 1012 (1956).
6. H. Lee, D. Stoffey and R. Neville, "New Linear Polymers", Chapter 8, McGraw Hill (1967).